International Journal of Disaster Risk Reduction 67 (2022) 102677

Contents lists available at ScienceDirect

International Journal of Disaster Risk Reduction

journal homepage: www.elsevier.com/locate/ijdrr

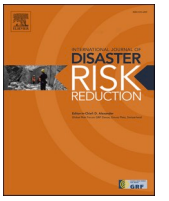

Neural networks for the rapid seismic assessment of existing moment-frame RC buildings

Lorenzo Stefanini [a], Lorenzo Badini [a,*], Giovanni Mochi [b], Giorgia Predari [a], Annarita Ferrante [a]

[a] Department of Architecture, University of Bologna, Bologna, Italy
[b] Department of Civil and Environmental Engineering, University of Perugia, Perugia, Italy

ARTICLE INFO

Keywords:
Reinforced concrete
Artificial neural network
Seismic vulnerability assessment
Damage prediction
Existing buildings

ABSTRACT

The study presented in this paper analyses and investigates the possibility of introducing a general and rapid methodology based on an artificial neural network (ANN) to assess the seismic response of existing reinforced concrete (RC) buildings. Starting from investigations carried out on buildings located in the outskirts of Bologna, 928 finite element models have been developed on the basis of the most recurrent data. The input parameters representing the characteristics of the structures were systematically varied and, through modal dynamic and non-linear static analyses, the outputs representing the seismic response were recorded. The resulting dataset was used to create a function, based on ANN, that can reliably predict the seismic behaviour of a RC structure. Finally, by means of k-fold cross-validation, the instruction of the function was optimised and simultaneously verified, obtaining a coefficient of determination for the totality of the samples and the previously unseen cases of 0,94 and 0,88, respectively. The result obtained not only aims at enriching the existing framework on the subject, increasing the awareness of the seismic issues affecting this building typology, but also constitutes a prioritization system that could highlight the need for structural renovation.

1. Introduction

Seismic hazard is a relevant topic for the whole Mediterranean area [1]. Over the years, experts and researchers have devoted their efforts to develop new intervention and prevention strategies. In this continuous evolution, even if construction standards and techniques have been developed towards a progressive improvement of the design and construction phases, most of the European real estate heritage predates the latest technological achievements and modern seismic regulations, resulting in a widespread seismic risk. Among all building typologies, this study focuses on reinforced concrete (RC) residential buildings built between the second half of the 20th century and the early 1990s, potentially characterized by structural criticalities, as reported in §1.2.3 of deliverable D.2.2 [2].

In this context, the use of a methodology to assess the seismic response of these structures in a reasonable time and with a good degree of accuracy is increasingly important. Especially because of the financial and time constraints associated with the use of detailed damage assessment methods on numerous buildings [3,4].

With the aim of sharing knowledge on vulnerability assessment and discussing limitations and possible improvements of the know-how, a group of 12 experts from academia, engineering and disaster risk modelling community met in Pavia (Italy) in 2017 [5]. They

* Corresponding author. Department of Architecture, University of Bologna, Viale Risorgimento 2, Bologna, 40100, Italy.
E-mail address: lorenzo.badini3@unibo.it (L. Badini).

https://doi.org/10.1016/j.ijdrr.2021.102677
Received 16 April 2021; Received in revised form 6 October 2021; Accepted 3 November 2021
Available online 16 November 2021

stated that over the last three decades, dozens of methodologies have been proposed for the analytical derivation of fragility and vulnerability functions, with different levels of complexity and accuracy. Notable among the factors that mainly determine these assessment methods are the strong motions used, the availability of data on existing buildings and finite element modelling (FEM). Two approaches seem to be predominant in this context: one that investigates the seismic vulnerability using multi-degree-of-freedom (MDOF) models of few most representative buildings (chosen from a much larger population as index buildings) and a second way that involves more simplified models with only a single degree of freedom (SDOF) [5]. A distinction is then made on two sources of variability: intra-building and inter-building variability. The first refers to variability within the building, mainly caused by uncertainty in building properties, FEM, and analysis method; the simpler the modelling approach (and the less data available), the more uncertain the index building results will be. The second relates to the typical variability of each construction. It is easier to have greater variability between different buildings of the same class than between different plausible models of a given structure. Consequently, quantity is promoted with the hope that sampling multiple types will capture the dominant inter-building variability, while reduced-order models and simplified analysis approaches may consistently compromise the assessment results, thus not only adding some additional uncertainty, but also shifting the estimated vulnerability to higher or lower values [5].

The need for rapid screening of existing buildings was first recognized by a group of researchers in Italy [6–9]. On the basis of the analyses developed by Benedetti and Petrini, the National Group for the Defence of Earthquakes (in original language *Gruppo Nazionale* per *la Difesa dai Terremoti,* GNDT) created in 1994 a series of data sheets [10], used to give an immediate evaluation of the state of existing buildings after the occurrence of an earthquake as a damage and preventive vulnerability assessment.

After the Irpinia earthquake of November 23, 1980, a catalogue of about 30.000 buildings in over forty municipalities was collected to define Damage Probability Matrices (DPMs) [11–13]. The purpose of those matrices was to estimate the probability that a given building would suffer damage from an earthquake. DPMs have been used, more recently, on a sample of masonry churches in Italy [14]. These matrices were associated with each collapse mechanism present for each case study and combined to obtain a vulnerability index for the individual church. Based on these data, it was possible to statistically analyse the entire sample. The researchers introduced binomial probability distribution functions (BPDFs), which express the fragility prediction of the sample, in combination with DPMs. The method produced a large-scale post-earthquake assessment tool in terms of fragility and vulnerability prediction that can prioritize buildings for retrofit. The disadvantage of DPMs is a great effort in terms of time and costs to create a dataset that covers only a small part of the building types present on the territory. Another method for seismic assessment of RC and masonry structures has been developed at the University of Bologna: RE.SIS.TO Ref. [15]. This procedure was inspired by existing methods in the literature [10] to assess vulnerability on a large-scale. It leads to the definition of a peak ground acceleration (PGA) value, corresponding to the collapse of the building, through the calculation of its shear strength. This parameter is evaluated using simplified mechanical considerations that require a preliminary technical opinion from an expert to summarise the real complexity of the construction without losing accuracy.

In recent years, analysts have introduced rapid visual screening (RVS) methods with the aim of prioritising buildings at higher seismic risk and assisting decision makers in implementing preventive strategies. RVS methods are based on questionnaires, usually completed by experts, in which the main characteristics of buildings are collected and processed to define a seismic risk index [16,17]. Many countries have adopted these procedures as initial tools to identify the most vulnerable buildings and often focus on certain classes or types of buildings such as hospitals [18] or schools [16]. These processes require reporting on the choices made in the simplification phase and the data included in the assessment. In the RVS method presented by Ruggieri et al. [14,16]; the focus was on school buildings in the Apulia region (southern Italy), most of which were undersized RC structures with three or fewer floors. The specific questionnaires were focused on a selection of parameters that well represented the class under investigation, considering both structural and non-structural elements. The RSV result attempts to represent the social and economic losses that might follow major earthquakes and is a combination of the three main parameters that make up seismic risk: 1) seismic hazard of the region; 2) exposure of the affected areas; and 3) vulnerability of the structures [19]. As also reported by M. H. Arslan et al. [20]; this topic concerns most of the Mediterranean countries. On the Turkish experience, for example, many other contributions can be cited [21–24].

A problem encountered when analysing classical evaluation methodologies is that the accuracy of the results is sacrificed in favour of the speed of data processing, or vice versa, hardly managing to combine the two aspects simultaneously. Moreover, these methods are often based on expert consultancy, which, as has been shown in various fields (starting with behavioural psychology), is usually the much less preferable predictive system in noisy environments [25,26].

Tools that are now widely used in research to describe complex relationships influenced by certain parameters are Artificial Neural Networks (ANNs). ANN is a type of artificial intelligence application that has already been used by engineers in the building sector for many purposes: prediction of various structural quantities [27–31], diagnosis and detection of structural damage [32–34], active response control of offshore structures [35,36], identification of the static model of an FRP deck [37] etc. Investigations have also been made in the last decades to evaluate the performance of existing RC structures [20,38–41]. In particular, after an evaluation of effective design parameters on seismic performance of existing RC buildings [38,39], M. H. Arslan et al. [20] proposed a rapid evaluation method based on ANNs to determine their performance level. They characterised the dataset to match the typical properties of the Turkish building stock and made specific reference to the national seismic code. Using a linear structural analysis approach applied to three-dimensional FEM models, they determined the performance level of a building by quantifying the damage for each structural element and considering the percentage of those that were beyond a certain state. Vazirizade et al. [41] used ANNs in reverse: to determine the degree of damage of a structure (location and extent) they started from the structural response of two-dimensional (2D) steel frames.

With the same scheme, using non-linear time history analyses on 2D-RC frames and damage indices, de Lautour and Omenzetter [40] obtained an ANN capable of predicting damage with a good approximation for cases within the range of input properties.

In this study, a similar approach is proposed: 37 different values, divided into mechanical, construction, and morphological parameters, were selected to parameterize a generic RC moment-resisting frame structure (inputs). Then, non-linear static FEM (push-over) and modal dynamic analyses were performed, recording 17 independent structural response values (outputs) on a sample of 928 different models. As described in previous studies (M. H [20,40]. parameterization of the sample is necessary to create a neural network. In their study, De Lautour and Omenzetter [40] introduced 19 parameters describing structural properties and ground motions, obtaining an output vulnerability with damage indices. H. Arslan et al. [20] provided the same number of parameters, first describing the horizontal loads (reference acceleration and soil type) and then the building characteristics. In this case, the output entered in the dataset is directly related to the Turkish standard and represents a performance level.

The data set presented in this study is used to train a mathematical-informatics model based on a neural network, capable of extending the results obtained to real cases not yet included in the training database. Previous studies have shown that, compared to traditional methods, the characteristics of artificial neural networks (ANNs) and their learning capacity are very well suited to the purpose [42]. Moreover, the results obtained through this system in various domains seemed encouraging. Morfidis and Kostinakis [43]; Ferreira et al. [44] and the approach adopted by Estêvão [45] constitute excellent examples of ANN applications in the field of structural engineering and seismic assessment. As illustrated by Abbes Berrais [46]; the main advantages of this approach are the ability to gain experience through self-training, the resistance to errors and uncertainties and the ability to extract information from noisy and incomplete databases. Although a comparison between regression methods is not the purpose of this research, which is limited to testing the applicability of neural networks for the definition of a rapid method of structural evaluation, some tests carried out with traditional systems, and reported in Appendix B, highlight their non-applicability to the problem in question.

The procedure, as illustrated in this text, aims to investigate the possibility of introducing a new type of RVS method that does not require a direct survey of a large number of typological buildings, but that, knowing the weight of some characteristic parameters, can preventively predict dangerous events for RC moment-resisting structures and therefore prioritize possible interventions. It is important to note that the inputs are selected in such a way as to univocally represent the morphology of a RC building, allowing, in further phases of the research, to implement the reference database, including building types different from the most recurrent ones in the specific area reported in this study [47,48].

2. From building data to parameters

In order to start collecting data for the formulation of the method, a peripheral area of Bologna was identified that presented a good recurrence of buildings respecting the typology of interest of the study: residential buildings in RC constructed between the 1950s and 1990s. During that period in Italian and European cities, the growing demand for housing led to the formation of suburbs, often favouring quantity over quality and efficiency. These suburbs are therefore characterized by recurring structures and building technologies that can be generalised on the basis of a prior study of the detail. Therefore, in order to cover most of these recurring structural typologies in RC with a small number of FEM models, targeted investigations were conducted on a small sample of the existing building stock. This choice allowed to receive feedback on the performance of the system, not precluding the possibility of expanding the database to other building types in future updates. In fact, the parameters were chosen in such a way as to allow, in successive phases, the inclusion of structures with configurations very different from those analysed in this study.

The data was collected through two surveys with different objectives: the first, broader and more general, aimed at obtaining the most common planimetric shapes, the second, more specific, investigated the geometric characteristics of each building.

2.1. Data collection performed on case study

The first survey covered three areas of Bologna: Corticella, Emilia Levante and Emilia Ponente. The study analysed 1.051 constructions using the municipal technical cartography. This provided a first orientation on the configuration of the structures populating the database of the study [47,48]. The result was that 68,8% of the total building stock belongs to the square or rectangular shape (Table 1).

The second survey covered an area of Bologna bounded to the east by the motorway line and to the south by the railway line (see Fig. 1). From this sample the information for the creation of the FEM models was obtained. The analysis on cadastral plans indicated that 91,6% of the buildings were built before 1970, and 45,8% of those analysed are in RC. The following maps show graphically some of the data collected in the second survey area.

Due to the lack of specific information (structural drawings) concerning all the buildings surveyed, the data collection covered all the buildings in the area, including masonry or hybrid structures. The survey, as showed in Table 2, determined some geometric recurrences, including storey heights, span dimensions, plan configuration and column dimensions.

From this analysis it was possible to derive specific data, related to RC buildings, useful for the definition of reference structures:

- 84,6% of the buildings fall into a rectangular shape compared to 7,7% of square shaped cases;
- almost all buildings have a 3-bays structural scheme in the y-direction. The central span is always the shortest (Yb in Fig. 2), while the two side spans, sometimes equal and sometimes different, are the longest (Ya and Yc in Fig. 2);

Table 1
Results of the first survey – Shape recurrences.

Shapes	Rectangular	Square	T	L	C	S	Combined	Other
Percentage	20,20%	48,60%	4,20%	8,90%	3,50%	2,10%	2,20%	10,30%

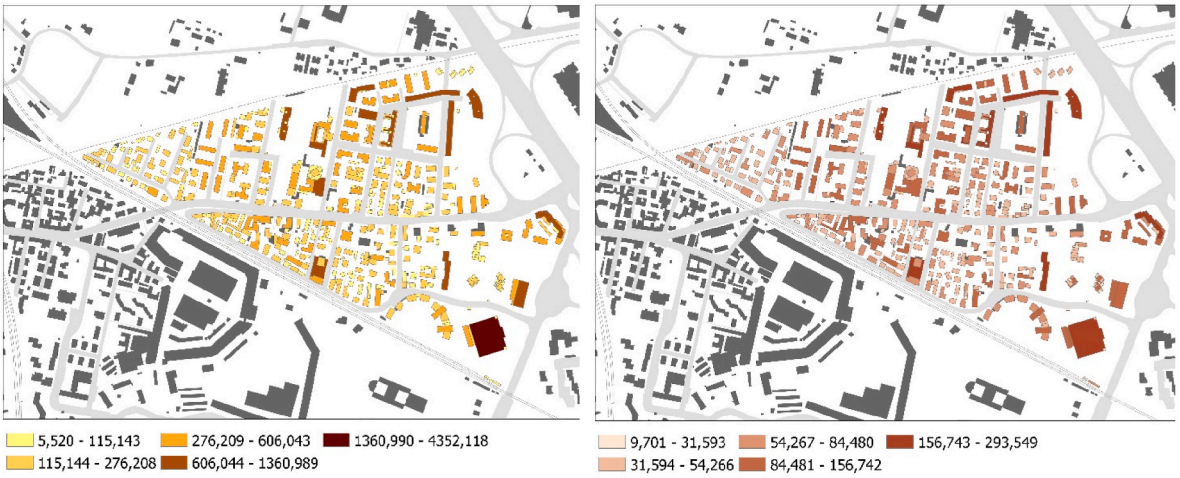

Fig. 1. Results from the second survey. The area of the buildings (m^2) and the perimeter (m) are represented on the left and right respectively.

Table 2
Results from the second survey. Collected parameters divided in (1), values with associated percentages, and (2), statistical data.

Collected parameters (1)									
Period of construction	%	Type of structure	%	Shape of the building	%	Area of the building	%	Perimeter of the building	%
1939–1955	37,5	Concrete	45,8	Rectangular	62,5	5,5–115,1	52,1	9,7–31,5	24,5
1956–1969	54,1	Masonry	33,3	Square	20,8	115,1–276,2	32,3	31,5–54,2	37,3
1970–1986	8,4	Hybrid	20,1	Other	16,7	276,2–606,0	12,9	54,2–84,5	22,6
–	–	–	–	–	–	606,0–1.360	2,5	84,5–156	12,7
–	–	–	–	–	–	1.360–4.352	0,2	156–293	0,3

Collected parameters (2)														
N. of floor			Inter-storey height (m)			Span x-direction (m)			Span y-direction (m)			Columns dimension (m)		
Min	Max	Avg	Min	Max	Avg	Min	Max	Avg	Min	Max	Avg	Min	Max	Avg
3	22	6,4	2,1	4,0	3,05	4,0	5,6	4,9	3,6	6,5	5,3	25 × 25	45 × 45	30 × 30

- the maximum span in the y-direction (distance between the frames) range from a minimum of 3,6 m to a maximum of 6,5 m;
- in the x-direction, buildings are generally made up of repeated modules that have a central staircase (usually a shorter bay, Xc in Fig. 2), flanked by larger spans (Xa, Xb). These spans vary in number from two to three and may be characterised by equal or different lengths;
- the length of the maximum spans in the x-direction (Xa and Xb in Fig. 2) are more variable with an average of about 5,3 m;
- the dimensions of the columns range from a minimum of 250 × 250mm to a maximum of 450 × 450 mm, which is the case only on the lower floors. The most frequent dimensions are 250 × 250 and 300 × 300 mm;
- the number of floors varies from 3 to 8 (with one tower of 22 floors, removed from the analysis), with an average value of 6,4. The recurrent typology has a basement and 3 or 4 floors above it;
- the standard height of the storeys is 3 m, with lower values for basements (h = 2,65 m) and higher values for ground floors (h = 3,40 m);

The mechanical characteristics, the amount of reinforcement and the construction details, not being obtainable without instrumental tests, were assumed on the basis of the technical standards in force at the time.

It is however important to emphasise that the investigations and the use of the codes served only to optimise the procedure and as a starting point: any discrepancies between the real building and the mechanical characteristics assumed do not invalidate the study carried out, which investigates the possibility of introducing a rapid methodology based on an artificial neural network and not on the structural evaluation of existing buildings.

2.2. Input parameters

The generation of an algorithm through ANN requires the definition of some parameters suitable to describe the problem to be examined, in this case an RC structure. The 37 selected values were chosen among those that bests describe the structural specificities of the building category (M. H. [38,49], remaining in a small number to avoid complicated network resolutions. From this perspective, it was decided to link some parameters to others (e.g., the dimensions of the main beams with those of the edge beams). The inputs

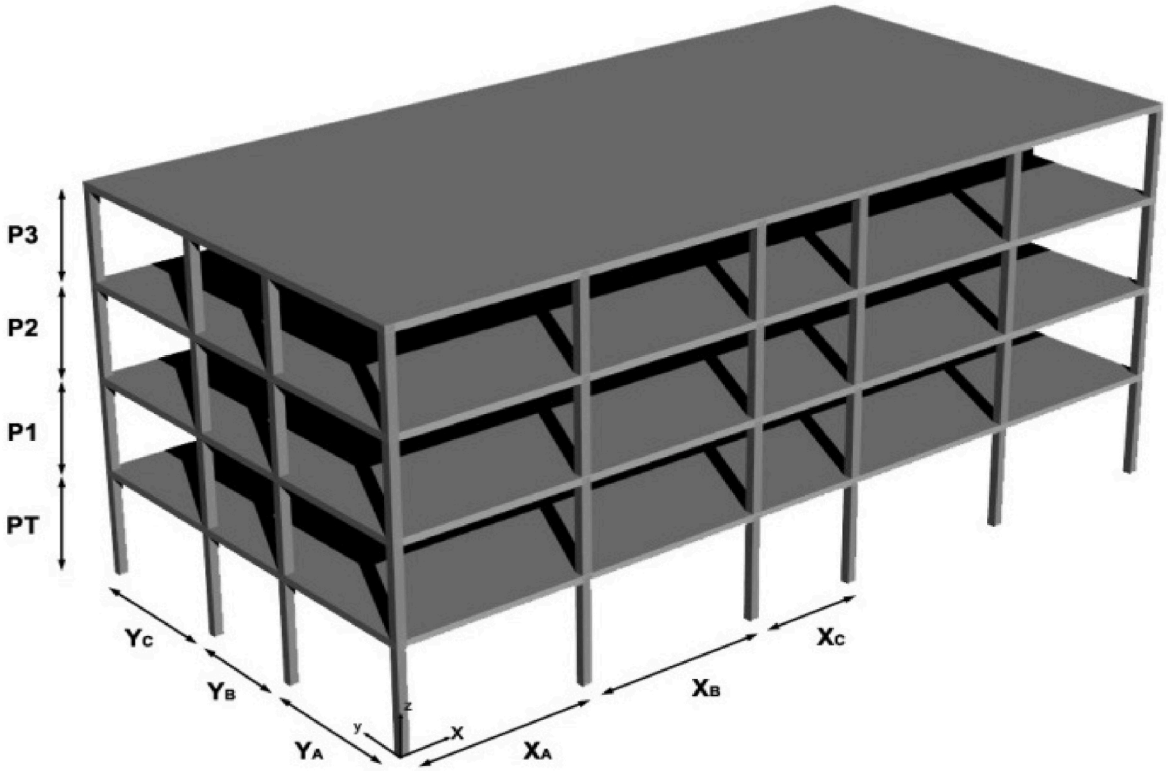

Fig. 2. Scheme of the recurring structure.

were divided into three general categories: mechanical, construction, and morphological parameters.

Mechanical parameters describe the characteristics of the structural materials. The construction parameters define the proprieties of the lateral resisting elements (e.g., column dimensions, reinforcements, etc). A change in a single input does not imply a change in the value of the other parameters in the same category, they are independent (for example, it is possible to change the size of a column without changing its reinforcements). Morphological parameters characterize the different forms assumed by the structure of buildings (e.g., spans, height, number of floors, etc.), and are dependent on each other: a variation on one of them implies a variation of several inputs of the same category (e.g., it is impossible to change the area of a building without changing its perimeter, base sides, etc.).

Although the study conducted is limited to a particular type of building, the selected parameters could characterize any structure, including irregular ones. Table 3 shows all the parameters (and their description) considered in the creation of the database. A range of values is also given, identifying the maximum and minimum. In Appendix A, all the variations considered between the threshold are shown.

2.3. Output parameters

The output parameters are the most important results obtained from the modal dynamic and non-linear static analyses (see Table 4). They constitute essential information on the behaviour of the structure and provide an estimate of the vulnerability level.

For the purpose of the study conducted and the correct training of the network, independent structural response parameters were chosen. It should be noted, however, that from this information it is possible to obtain, for a professional, other significant values such as the behaviour factor and the acceleration at various limit states.

3. The index structures: FEM, analyses and variations

In order to obtain the information needed to fill the database, it was necessary to start from geometrically and mechanically defined structures. Taking into account the results of the above investigation, four recurring geometrical and morphological solutions were chosen. With these, eight index (or reference) structures (IS) were determined through two dimensioning processes: the first one based on outdated normative requirements [51–53] using the permissible-stress method (IS1-4); the second one based on recent requirements [54], using the semi-probabilistic limit state method (IS5-8). This decision was taken in order to extend the prediction capacity of the system.

From these ISs, the input values in the FEM were varied systematically. Modifying one parameter at the time, leaving the others unchanged and recording the outputs. When all possible variations of a single parameter had been completed, then two or three parameters were modified simultaneously.

Table 3
Input parameters of the data set.

	Name and description	Range of values	U.M.
Mechanical Parameters			
1	**Concrete class (R_{ck})** Cubic characteristic compressive strength.	10–60	N/ mm^2
2	**Steel grade (f_{yk})** Characteristic tensile yield strength.	220–450	N/ mm^2
Construction Parameters			
3	**Columns dimension in x direction (C_x)** Measurement of the side of the column in x-direction.	0,25–0,60	m
4	**Columns dimension in y direction (C_y)** Measurement of the side of the column in y-direction.	0,25–0,60	m
5	**Longitudinal reinforcement bars in columns ($A_{s,c,long}$)** Amount of longitudinal reinforcement in columns, expressed in mm^2	452–4.562	mm^2
6	**Stirrups in columns ($A_{s,c,trans}$)** Amount of stirrups in columns, value expressed as mm^2 per meter.	226–5.655	mm^2/ m
7	**Columns variation per floor (ΔC)** The value considers whether the columns vary in section depending on the floor level or not. (0) Indicates a structure with all columns equal, (1) indicates a reduction, for each floor following the ground floor, of 50 mm on each side of the element, with a minimum of 250 mm.	0–1	–
8	**Main beam height (h_{mb})** Height of the main beams. Where the main beam is the internal beam, part of the moment-resisting frames.	0,35–0,7	m
9	**Main beam width (b_{mb})** Width of the main beams. Where the main beam is the internal beam, part of the moment-resisting frames.	0,20–0,50	m
10	**Longitudinal reinforcement bars in beams ($A_{s,b,long}$)** Amount of longitudinal reinforcement in beams, expressed in mm^2.	282–1.582	mm^2
11	**Stirrups in beams ($A_{s,b,trans}$)** Amount of stirrups in beams, value expressed as mm^2 per meter.	703–1.727	mm^2/ m
12	**Cracking (w)** The value takes into account the presence or absence of cracking in the resisting elements with reference to the percentages recommended in Eurocode 8 (CEN 2004c). (0) Elements have full shear and bending stiffnesses, (1) they have moduli reduced by half.	0–1	–
13	**Live loads (LL)** The value expresses the accidental loads considered in the calculations. It is expressed in kN/m^2.	2–4	kN/m^2
14	**Floor joist direction (F_{jd})** The value indicates the direction provided to the joists and, consequently, to the moment-resisting frames. (0) For joists deformed in y-direction, (1) for joists in x-direction.	0–1	–
15	**Secondary beams ($2^{nd}B$)** The value considers the presence or absence of secondary beams. Secondary beams connect the main frames in orthogonal direction. (0) if absent, (1) if present.	0–1	–
16	**Diaphragm constraints (DC)** The value indicates the presence or absence of the rigid diaphragm. (0) If absent, (1) if present.	0–1	–
Morphological parameters			
17	**Building Area (BA)** Geometric area enclosed by the perimeter line of the building.	120–300	m^2
18	**Perimeter (BP)** Length in meters of the perimeter line of the ground floor plan.	44–72	m
19	**Min. Moments of inertia of the plan (J_{min})** The parameter describes the minimum moment of inertia of the plane figure formed by the building plan with respect to the two main axes.	1.440–13.180	m^4
20	**Max. Moments of inertia of the plan (J_{max})** The parameter describes the maximum moment of inertia of the plane figure formed by the building plan with respect to the two main axes.	928–4.210	m^4
21	**Columns number (N°C)** Number of columns on the ground floor.	12–24	–
22	**Minimum span x ($l_{x,min}$)** The parameter defines the minimum centres distance between two columns with respect to the x direction.	3	m
23	**Maximum span x ($l_{x,max}$)** The parameter defines the maximum centres distance between two columns with respect to the x direction.	4,5–6,5	m
24	**Minimum span y ($l_{y,max}$)** The parameter defines the minimum centres distance between two columns with respect to the y direction.	3–4	m
25	**Maximum span y ($l_{y,min}$)** The parameter defines the maximum centres distance between two columns with respect to the y direction.	5–7	m
26	**Average span x ($M_{l,x}$)** The parameter defines the average centre distance between columns in x direction.	4–5	m
27		4,1–5,3	m

(*continued on next page*)

Table 3 (*continued*)

	Name and description	Range of values	U.M.
	Average span y ($M_{l,y}$) The parameter defines the average centre distance between columns in y direction.		
28	**Standard deviation of spans x ($\sigma_{l,x}$)** Index of the span variability measurements in x direction.	0,7–1,4	–
29	**Standard deviation of spans y ($\sigma_{l,y}$)** Index of the span variability measurements in x direction.	0,75–2,09	–
30	**Regularity index x (IR_x)** Parameter that allows to detect irregularities in the structural mesh such as misaligned or missing pillars in x direction. It is calculated as the mean value of the normalised coefficients of variation, considering all spans in the x direction.	0,66-1	–
31	**Regularity index y (IR_y)** Parameter that allows to detect irregularities in the structural mesh such as misaligned or missing pillars in y direction. It is calculated as the mean value of the normalised coefficients of variation, considering all spans in the y direction.	0,71-1	–
32	**Floor number (N°St)** Number of floors in the building.	2–8	–
33	**Minimum inter-storey height ($h_{is,min}$)** Minimum inter-storey height of the building.	3-3,5	m
34	**Maximum inter-storey height ($h_{is,max}$)** Maximum inter-floor height of the building. Usually the ground floor.	3,5	m
35	**Average inter-storey height ($M_{h,is}$)** The parameter defines the average inter-floor height.	3-3,5	m
36	**Standard deviation of the inter-storey height ($\sigma_{h,is}$)** The parameter defines the standard deviation of the inter-storey heights	0-0,25	–
37	**Height of the building (H_{tot})** The value describes the total height of the building.	6,5–24,5	m

3.1. Dimensioning of the index structures

As mentioned above, the first dimensioning approach used for the reference structures was based on outdated standard requirements and the permissible-stress method. After defining the morphology of the structures (see Table 5 and Fig. 3), the first four ISs were dimensioned as follows. The available codes were applied with respect to the minimum requirements given and, due to the performance orientation of some standards compared to others, the lowest and least demanding values were selected from all outdated standards and not exclusively from a particular one.

1. The slab thickness was determined as 1/25 (≥1/30, [51]) of the maximum span. Then, given the Italian context, a concrete slab of 4 cm and hollow lightning bricks were assumed. Then, the permanent loads applied on the floors were related to the maximum span, the imposed load was fixed for the category at 2,5 kN/m^2 and the live loads were established depending on the use of the floors, as indicated by the Eurocodes [55]. Diaphragm constraints were entered into the model and assigned to all the points belonging to the same plane, depending on the presence or absence of the parameter.
2. Once the storey loads were determined, it was possible to evaluate, through the area of influence, the design loads for the internal beams (main beams). The latter, horizontal elements of the RC frames, were only provided in one of the two main directions (depending on the relative parameter), leaving the connection in the opposite direction to the kerbs (when the secondary beam parameter was "activated"). These main beams were sized according to the maximum moments affecting their ends, which are $ql^2/10$ at the roof level and $ql^2/12$ at lower levels, where q is the distributed load and l is the length of the element. The dimensions of the cross-section and the amount of tensioned reinforcement were determined on the basis of stresses considering a fixed concrete cover of 3 cm. The compressed reinforcement was evaluated as 30% of the tensioned reinforcement. A verification of the stresses on both sides of concrete and steel was finally carried out considering the homogenised steel/concrete section (n = Es/Ec, [51]). The transverse reinforcement was evaluated as minimum percentages per meter (mm^2/m) in relation to the dimensions of the beams [53].
3. The kerbs (or secondary beams) were applied in the alternative direction of the main beams and were square in shape, depending on the height of the floors, with a minimum reinforcement content of 4φ12 in the longitudinal direction and φ6/30 in transversal direction [52].
4. The edge beams, located on the perimeter of the building, are subjected to half of the loads assigned to the main beams, as they are affected by half of the reference area. In addition, linear loads have been added to represent the external masonry infill walls, which are 25 cm thick. The dimensions of the edge beam cross-section were derived as a function of those of the main beam with a proportion of the applied loads. The longitudinal and transverse reinforcements were determined in the same way.
5. The cross-sectional dimensions of the columns were defined on the basis of the compressive strength of the concrete at ground level. The stresses, evaluated as the ratio of the maximum axial load and the area, were compared with the maximum compressive strength of the concrete reduced by 30%, due to the combination with the flexural actions. The longitudinal reinforcement was calculated as 0,8% of the concrete cross-section strictly necessary to meet the resistance to axial loads [51]. The transverse reinforcements are φ6/25 based on the worst condition presented in outdated standards prescriptions [52]. The columns of the reference structures (1–4 IS) have the same dimensions for the whole height of the building.

Table 4
Output parameters of the data set.

Description	N°	Acronym	Specification	U. M.
Output Parameters				
Base shear at the base for limit state: *limit states of damage limitation, significant damage and near collapse defined in accordance with the Eurocode 8 – Part 3* [50].	**1**	$\mathbf{V_{LS\text{-}DL\text{-}x}}$	Damage limitation in x directions	kN
	2	$\mathbf{V_{LS\text{-}DL\text{-}y}}$	Damage limitation in y directions	kN
	3	$\mathbf{V_{LS\text{-}SD\text{-}x}}$	Significant Damage in x directions	kN
	4	$\mathbf{V_{LS\text{-}SD\text{-}y}}$	Significant Damage in y directions	kN
	5	$\mathbf{V_{LS\text{-}NC\text{-}x}}$	Near Collapse in x directions	kN
	6	$\mathbf{V_{LS\text{-}NC\text{-}y}}$	Near Collapse in y directions	kN
Activated mass: *depends on the fundamental mode of vibration.*	**7**	$\mathbf{m^*_x}$	Activated mass in x directions	kg
	8	$\mathbf{m^*_y}$	Activated mass in y directions	kg
Displacement to the limit state: *maximum displacement registered at the roof-floor during the pushover analysis.*	**9**	$\mathbf{d_{LS\text{-}DL\text{-}x}}$	Damage limitation in x directions	mm
	10	$\mathbf{d_{LS\text{-}DL\text{-}y}}$	Damage limitation in y directions	mm
	11	$\mathbf{d_{LS\text{-}SD\text{-}x}}$	Significant Damage in x directions	mm
	12	$\mathbf{d_{LS\text{-}SD\text{-}y}}$	Significant Damage in y directions	mm
	13	$\mathbf{d_{LS\text{-}NC\text{-}x}}$	Near Collapse in x directions	mm
	14	$\mathbf{d_{LS\text{-}NC\text{-}y}}$	Near Collapse in y directions	mm
Fundamental period of the structure: *first two periods bending the structure in the two main directions. Evaluated with the modal analysis.*	**15**	$\mathbf{T_x}$	Fundamental period in x directions	s
	16	$\mathbf{T_y}$	Fundamental period in y directions	s
Vulnerability index: *ratio between the plastic hinges formed in the pre-seismic phase and the total hinges of the building. The value was specially designed for this study so that even structures not verified for vertical loads could be evaluated.* *In fact, pushover does not allow distinctions to be made between buildings in which critical values are already reached for vertical loads, since the values of the base shear and displacements are 0.* *The vulnerability index can assume values between 0 and 1, where 0 means no flexural criticality for vertical loads (the most common case). Therefore, in the case of buildings in which the parameter takes on values other than 0, the structure with the highest index can be assumed to be the most vulnerable.*	**17**	**I**	Vulnerability index	–

6. The curtain walls, not being assignable to fixed categories due to their great variability (presence or absence of windows, type of material, etc.) have been considered only from the point of view of transferred loads.

The resulting index structures (1–4 IS) are characterised by very low collapse acceleration values and show premature initiation of brittle mechanisms (shear failure of beams or columns). In this type of buildings, the strength hierarchy is often not respected and even improving the values of one or more parameters does not lead to significant results in terms of seismic response. Although these buildings represent well the majority of the existing building stock, they hardly simulate the behaviour of structures with a more ductile behaviour and a lower vulnerability level. Therefore, in order to include this case in the research and to improve the prediction possibilities of the network, four additional high-performance models with the same morphology as the previous ones, but dimensioned on the basis of more recent Italian regulations [54], have been developed. Moreover, in order to obtain models with the desired characteristics, the response spectrum of the city of L'Aquila, where the ground acceleration is one of the highest in Italy, was used for the dimensioning of the structures (5-8IS).

The design of the reinforcements was then carried out directly with the FEM software on the basis of the requirements of NTC2008 [54] (the latest Italian code available for the RC design in the software at the time of the analysis). Given the regularity in plan and elevation of the reference structures, a q-factor of 3 was used. The elastic and design response spectra applied in the analyses are shown in Fig. 4. Table 6 shows all the mechanical and construction parameters for IS 1 to 8.

3.2. FEM and seismic analyses

The 17-output data were provided by numerical analyses using FEM. For this purpose, SAP2000 [56] was used.

The class of concrete and the grade of the steel were computed in the model. The former is automatically provided by the software database, already characterised by a specific value of compressive strength and modulus of elasticity, depending on the class

Table 5
Morphological parameters implemented in the database and representing the eight index structures (IS) evaluated in the study.

Morphological parameters	Units	IS1 – IS5	IS2 – IS6	IS3 – IS7	IS4 – IS8
BA	m^2	130	230	169	299
BP	m	46	66	52	72
J_{min}	m^4	1083	1917	2380	4211
J_{max}	m^4	1831	10139	2380	13181
N°C	–	12	24	16	24
$l_{x,max}$	m	5	5	5	5
$l_{x,min}$	m	3	3	3	3
$M_{l,x}$	m	4,33	4,6	4,33	4,6
$\sigma_{l,x}$	–	0,94	0,8	0,94	0,8
IR_x	–	1	1	1	1
$l_{y,max}$	m	6	6	5	5
$l_{y,min}$	m	4	4	3	3
$M_{l,y}$	m	5,0	5,0	4,33	4,33
$\sigma_{l,y}$	–	1	1	0,94	0,94
IR_y	–	1	1	1	1
N°St	–	5	3	5	3
$h_{is,max}$	m	3,5	3,5	3,5	3,5
$h_{is,min}$	m	3	3	3	3
$M_{h,is}$	m	3,1	3,17	3,1	3,17
$\sigma_{h,is}$	–	0,2	0,24	0,2	0,24
H_{tot}	m	15,5	9,5	15,5	9,5

concerned; the latter was entered manually for each structure that did not include B450C (examples of material stress-strain relationships are given in Fig. 5). It was therefore necessary to define customised reinforcement materials for the classes: FeB22k, FeB32k, FeB38k and FeB44k. The tensile yield strength, ultimate yield strength and maximum elongation were entered into the material characteristics in the software based on Table 7 (data collected from D.M. 1972 [52] and NTC 2008 [54]).

Three-dimensional models of each structure were created to perform the non-linear static analysis (pushover). Fixed joints were introduced at the basement level as external restraints to simplify the foundation level. Beam and column elements were modelled as non-linear frames with lumped plasticity defining plastic hinges at both ends of the beams and columns. The properties of the hinges follow the formulae given in Annex A of Eurocode 8-Part 3 [50] for ductile mechanisms (see (1), (2) and (3)), indicating the three performance levels (or limit states, LS) defined in the same standards as damage limitation (LS-DL), significant damage (LS-SD) and near collapse (LS-NC). As shown in Fig. 6, five points labelled A, B, C, D, and E define the force–strain behaviour of a plastic hinge with controlled deformation.

$$\theta_u = \frac{1}{\gamma_{el}} 0.016 \cdot (0.3^{\nu}) \left[\frac{max(0.01;\omega')}{max(0.01;\omega)} f_c\right]^{0.225} \left(\frac{L_V}{h}\right)^{0.35} 25^{\left(\alpha\rho_{sx}\frac{f_{yw}}{f_c}\right)} \left(1.25^{100\rho_d}\right) - LS\ NC \tag{1}$$

$$\theta_{SD} = \frac{3}{4}\theta_u - LS\ SD \tag{2}$$

$$\theta_y = \varphi_y \frac{L_V + a_v z}{3} + 0.0014\left(1 + 1.5\frac{h}{L_V}\right) + \frac{\varepsilon_y}{d - d'}\frac{d_{bL} f_y}{6\sqrt{f_c}} - LS\ DL \tag{3}$$

The values assigned to each of these points vary depending on the type and cross-section of the element, the material properties, the longitudinal and transverse steel reinforcement, and the level of axial loading on the elements calculated with a quasi-static combination of vertical loads. SAP2000 provides predefined hinge properties and recommends PMM hinges (combined flexural and axial loads) for columns and M3 hinges (only flexural loads) for beams. Once the structure is modelled with the properties of the section, the steel content and the loads on it, the default hinges are assigned to the elements (PMM for columns and M3 for beams).

In order to consider brittle failures on the same elements, force-controlled hinges have been placed at the centre of each column and at the ends of each beam (V2 for beams and V2–V3 for columns). The shear strength, which is the maximum permissible force for these elements, is calculated as the maximum value found by varying the angle θ (between 21,8° e 45°) to match the tensile shear strength (failure of the transverse reinforcement) with the compressive shear strength (failure of the compressed concrete rod). Formulas (4), (5) and (6) were used in this respect, with reference to § 6.2.3 of Eurocode 2 [57].

$$V_{Rd} = \min(V_{Rsd}; V_{Rcd}) \tag{4}$$

$$V_{Rsd} = z \cdot \frac{A_{sw}}{s} \cdot f_{ywd} \cdot \cot\theta \tag{5}$$

$$V_{Rcd} = z \cdot b_w \cdot \alpha_{cw} \cdot \frac{v_1 \cdot f_{cd}}{(\tan\theta + \cot\theta)} \tag{6}$$

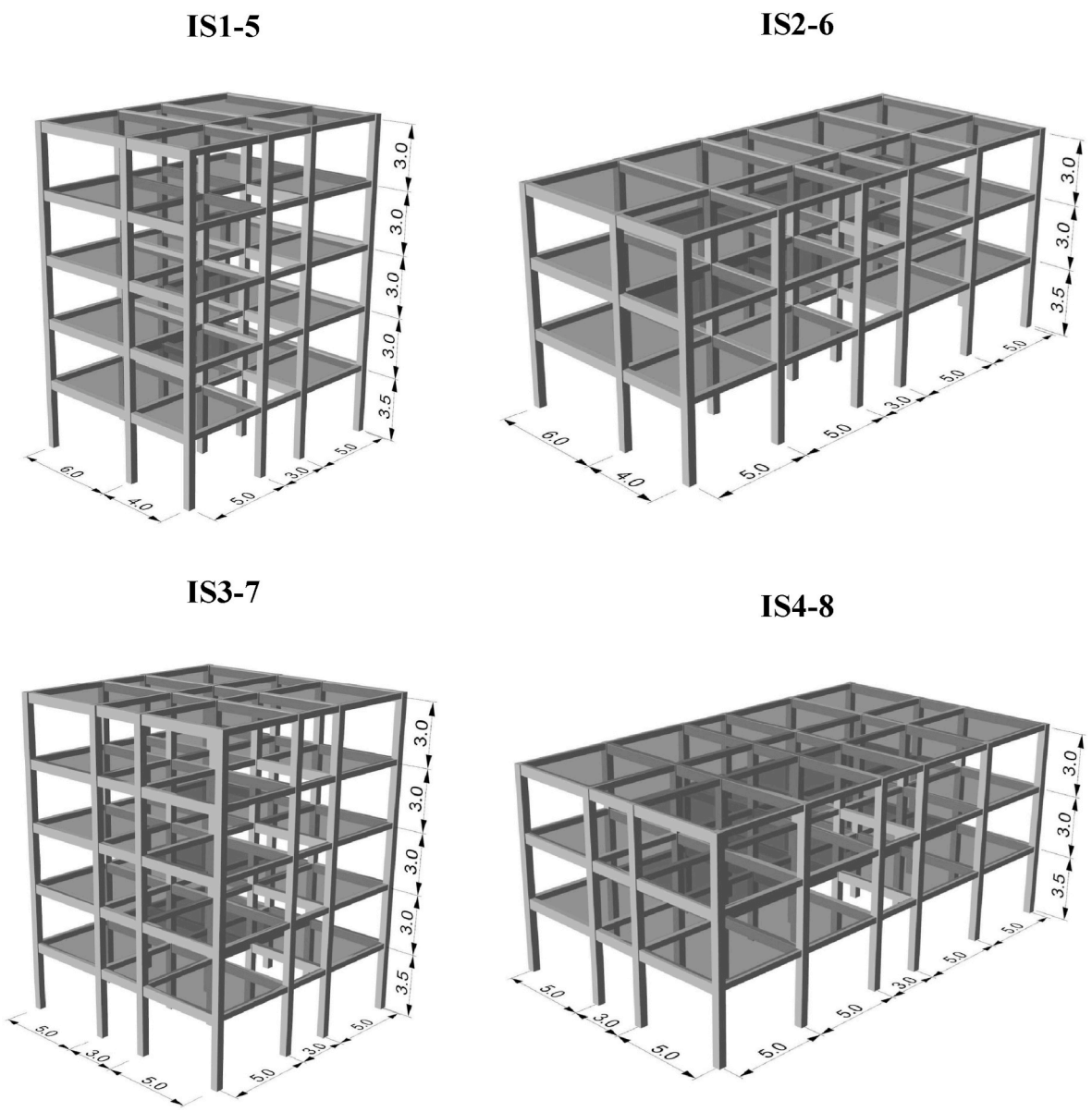

Fig. 3. Axonometric views of the FEM index structures determined on the basis of the geometrical recurring characteristics obtained from the surveys.

In this way, it was possible to consider all failure modes in the same pushover analyses. Thus, without neglecting axial and shear failures and avoiding fragility analysis errors [5].

Rigid diaphragm constraints, as described above, are inserted at each level whenever the case study presented a concrete slab of thickness greater than or equal to 4 cm. This constraint is applied at all the joints belonging to the same level. When the diaphragm constraint parameter was deactivated, the constraints in the model were also removed. Loads were divided into patterns and applied to two-dimensional elements with null cross-section distributing the loads in one or two directions, as required.

Regarding the analyses, a dynamic modal analysis and a non-linear static analysis were performed. The first required the definition of the mass source in the model characterised by a combination of load patterns with certain combination coefficients Ψ_{Ei}, as indicated in Eurocode 8 [58]. Twelve eigen modes were set as properties of the structures ensuring an activated mass greater of 90%. The activated mass and fundamental periods were recorded for each building studied.

A non-linear force-controlled static analysis, based on the quasi-permanent vertical load combination is the starting point for the two displacement-control pushover analyses performed in the two main horizontal directions with a force distribution proportional to the floor masses. Therefore, the capacity curves were extracted as results of the analyses (see Fig. 7), indicating the shear at the base in relation to the displacement of the control point (roof level). The exceeding of the limit states was then recorded in the capacity curves when a single plastic hinge exceeded the concerned limit. While the displacement-controlled plastic hinges allowed the progressive

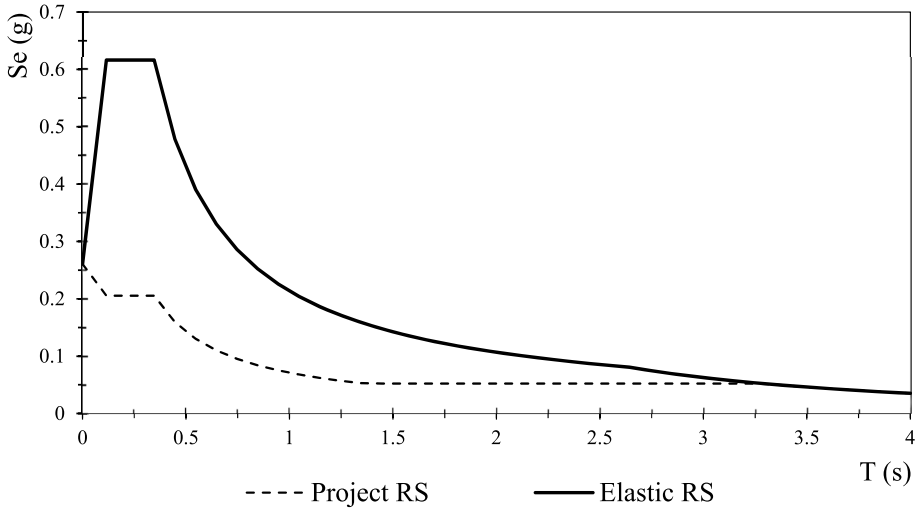

Fig. 4. Elastic response spectrum (E-RS) and project response spectrum (P-RS) located in L'Aquila, Italy.

Table 6
Mechanical and construction parameters representing the eight index structures (IS) evaluated in the study.

Mech. & Const. parameters	Units	IS 1	IS 2	IS 3	IS 4	IS 5	IS 6	IS 7	IS 8
$\mathbf{R_{ck}}$	N/mm^2	30	30	30	30	30	30	30	30
$\mathbf{f_{yk}}$	N/mm^2	315	315	315	315	450	450	450	450
DC	–	Yes	Yes	Yes	Yes	Yes	Yes	Yes	Yes
LL	kN/m^2	2	2	2	2	2	2	2	2
$\mathbf{F_{jd}}$	–	Y	Y	Y	Y	Y	Y	Y	Y
$\mathbf{A_{s,c,trans}}$	mm^2/m	226	226	226	226	1371	1035	1371	1169
$\mathbf{A_{s,c,long}}$	mm^2	1206	804	1206	804	4562	3770	4562	3770
$\mathbf{C_x}$	m	0,4	0,3	0,35	0,3	0,4	0,4	0,45	0,5
$\mathbf{C_y}$	m	0,4	0,3	0,35	0,3	0,4	0,4	0,45	0,5
ΔC	–	No	No	No	No	No	No	No	No
$\mathbf{A_{s,b,trans}}$	mm^2/m	1100	1100	1100	1100	1100	1280	1100	1340
$\mathbf{A_{s,b,long}}$	mm^2	983	925	807	847	1070	1070	983	983
$\mathbf{b_{mb}}$	m	0,3	0,3	0,3	0,3	0,3	0,3	0,3	0,3
$\mathbf{h_{mb}}$	m	0,5	0,45	0,4	0,4	0,5	0,45	0,4	0,4
$\mathbf{2^{nd}B}$	–	Yes	Yes	Yes	Yes	Yes	Yes	Yes	Yes
w	–	Yes	Yes	Yes	Yes	No	No	No	No

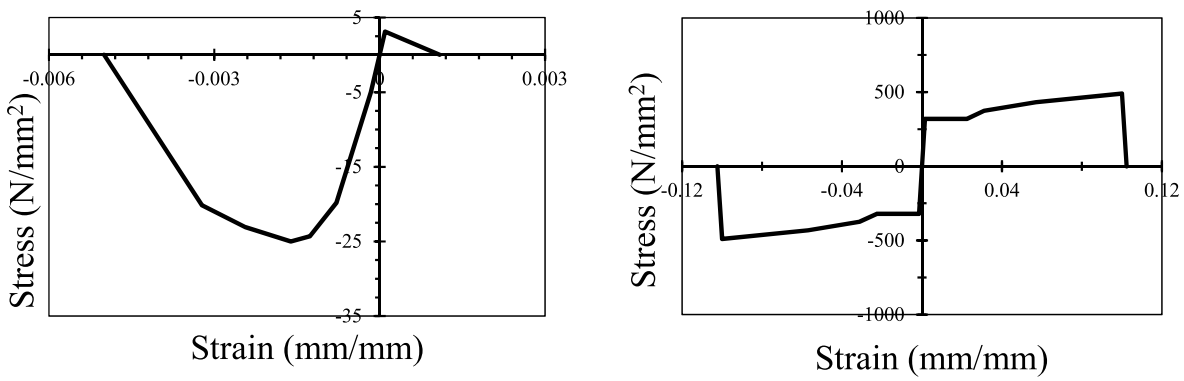

Fig. 5. Example of stress-strain relationships provided in the software for a C25/30 concrete class and a FeB32k steel grade.

damage of the structure to be recorded, going from LS-DL to LS-NC, the force-controlled plastic hinges directly indicated the collapse of the building, even if it was only determined by the vertical loads.

It is well-known that, in methods based on linear analysis, there is the conceptual limitation of considering the dissipative effects of the structures through the behaviour factor and therefore having to predict this parameter before carrying out the analysis. By using

Table 7
Mechanical properties of the steel grades considered in the FEMs. For each of the grades the reference standard is indicated in the table.

Steel grade	FeB22k	FeB32k	FeB38k	FeB44k	B450C
Tensile yielding strength f_{yk} ***MPa***	≥220	≥320	≥380	≥440	≥450
Ultimate yielding strength f_{tk} ***MPa***	≥340	≥500	≥460	≥550	≥215
Maximum elongation (A_s) %	≥24	≥23	≥14	≥12	≥7,5
Reference standard	DM72 [52]	DM72 [52]	DM72 [52]	DM72 [52]	NTC2008 [54]

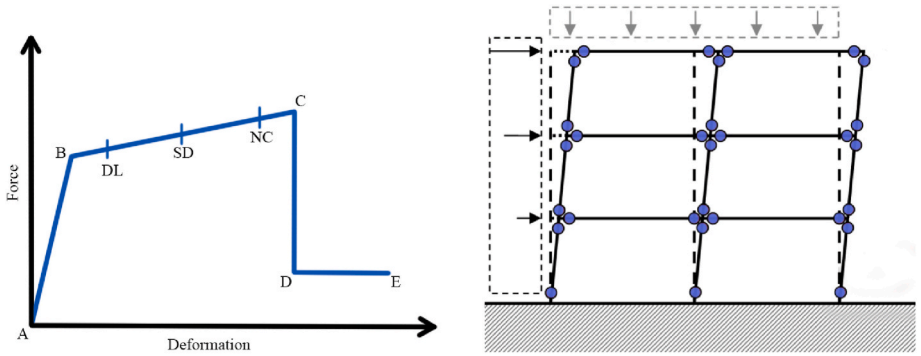

Fig. 6. On the left the back-bone curve provided for each deformation-controlled plastic hinges, with relative limit state limits (DL, SD and NC). On the right, a scheme representing the positioning of the deformation-controlled plastic-hinges on a frame.

non-linear analysis, this uncertainty can be avoided because the plastic behaviour of the elements is already predicted in the model. The pushover analysis considers the progressive deterioration of the structure during the earthquake through the non-linear behaviour of materials and plastic-hinges. In addition, a specific stiffness reduction in the resistant elements was considered to account for pre-existing cracks and possible failures related to the durability of the concrete. The bending and shear stiffnesses are both reduced by 50% in the beams, while in the columns by 30% (lower value due to the positive contribution of the axial load) and 50% respectively.

Due to the nature of this study, the capacity of the building has not been compared at this stage with the seismic demand to which it is subjected, as it is not relevant to the research. However, based on of the outputs provided by the proposed system, a user, at a later stage, could determine the vulnerability of the structure in relation to a demand value depending on the specific interested location.

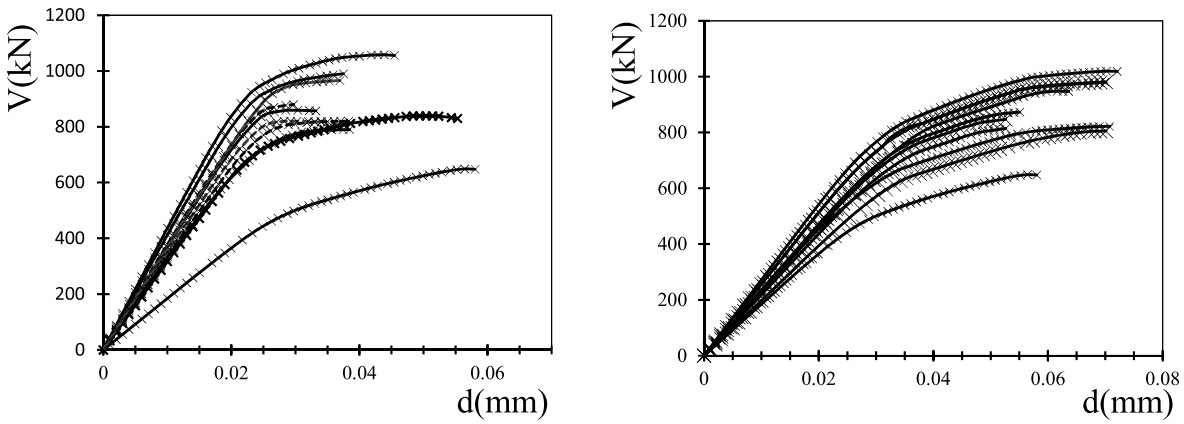

Fig. 7. The pushover curves for 10 buildings within the database are shown as an example. On the left the results obtained in the x-direction, on the right those in the y-direction.

In terms of acceleration, with reference to the nomenclature introduced by the *Annex to the Italian building code* (2019) [59]:

$$\zeta_E = \frac{a_{g,d}}{a_{g,c}} \leq 1 \tag{7}$$

with:

ζ_E structural vulnerability.

$a_{g,d}$ pseudo-acceleration obtained from the elastic response spectrum depending on the reference period.

$a_{g,c} = \frac{V_{max,LS}}{m^* \cdot g}$ collapse acceleration related to the exceedance of the limit state values by a plastic hinge (simplified procedure).

$V_{max,LS}$ maximum horizontal force for which at least one plastic hinge reaches the limit state considered.

m^* activated mass along that direction by the vibration mode.

The assessment made in (1) provides more conservative values than those that would be obtained with a rigorous target displacement verification as indicated by standards [58,60] since the ratio of accelerations does not fully consider the dissipative capacity of the structure. However, reinforced concrete constructions vulnerable to earthquakes are often affected by brittle failure due to reduced or incorrect arrangement of reinforcement. Future developments of the method will be aimed at providing outputs that can allow an assessment aligned with that of legislation, although the purpose of the rapid assessment (as a prioritization tool) is to provide values that conservatively represent vulnerabilities of buildings in a short period of time.

Table 8
Scheme representing the procedure used for varying the parameters. Specification is made on the models created in each phase.

Variation made	Parameters permutated				Total models
No Variation	Index Structures (ISs)				**8**
One Parameter at thr Time: *all the inputs in this row have been edited individually, starting from the ISs. They assumed the values considered in this study (see Appendix A), leaving the others in the initial configuration.*	Concrete Class	Steel Grade	Columns Dimension in X Direction	Diaphragm Constraints	**208**
	Longitudinal Reinforcement in Columns	Stirrups in Columns	Columns Variation Per Floor	Main Beam Height	
	Main Beam Width	Longitudinal Reinforcement in Beams	Stirrups in Beams	Edge Beams	
	Designated Use/ Imposed Loads	Floor Joist Direction			
Two Parameter at the Time: *all the inputs in this row have been edited in pairs, starting from the ISs. They assumed the values considered in this study (see Appendix A), leaving the others in the initial configuration.*	Concrete Class + Stell Grade	Concrete Class + Designated Use	Concrete Class + Cracking	Concrete Class + Columns Dimension in X	**352**
	Concrete Class + Long. Reinf. in Columns	Concrete Class + Stirrups in Columns	Concrete Class + Edge Beams	Edge Beams + Stell Grade	
	Edge Beams + Designated Use	Edge Beams + Columns Variation Per Floor	Edge Beams + Main Beam Height	Edge Beams + Main Beam Width	
	Edge Beams + Long. Reinf. in Beams	Edge Beams + Stirrups in Beams	Edge Beams + Long. Reinf. in Columns	Edge Beams + Stirrups in Columns	
	Stell Grade + Designated Use	Stell Grade + Cracking	Cracking + Designated Use	Cracking + Columns Dimension in X	
	Cracking + Floor Joist Direction	Cracking + Main Beam Height	Cracking + Main Beam Width	Cracking + Long. Reinf. in Beams	
	Cracking + Stirrups in Beams	Columns Dimension in Y + Columns Dimension in X			
Tree or more Parameter at the Time: *After the first 560 variations, three or more inputs were varied at the time. In particular: the morphological parameters (changing one implies changing the others e.g., the area and perimeter of the building) and the parameters that most commonly vary together (e.g., number of floors with pillar size and concrete class).*					**368**
Total Number of Models					**928**

3.3. Variations

Any neural network, in order to learn a given problem, must be trained on a sufficiently large number of case studies. Considering only the mechanical and construction parameters chosen, the models to be analysed to cover all the case studies would have resulted:

$$P_n = Ipt_1 \cdot Ipt_2 \cdot \ldots \cdot Ipt_n = 7 \cdot 4 \cdot 6 \cdot 6 \cdot 12 \cdot 13 \cdot 2 \cdot 8 \cdot 3 \cdot 8 \cdot 16 \cdot 2 \cdot 3 \cdot 2 \cdot 2 \cdot 2 = 46 \cdot 10^9 \tag{8}$$

where P_n is the total number of structures (considering only the mechanical and construction parameters) and Ipt_i is the number of configurations that a given input can assume among the chosen values (see Appendix A). In addition, the number reported does not consider the multiple shapes that buildings may take in plan. Therefore, the aim of this contribution, among the others previously mentioned, is to verify the method based on neural networks, highlighting that from a limited number of models it is possible to approximate reliable results for a much larger set of similar structures.

From the initial configurations illustrated above (IS 1–8) the inputs were varied, recording, for each modification, the relative outputs. The variation of morphological inputs is provided using the eight ISs together with a limited number of modifications specified in Appendix A. On the contrary, the mechanical, and construction parameters were punctually varied in different steps.

In particular, the first step of the procedure was to vary one parameter at a time, leaving the others unchanged, and then several parameters were varied simultaneously (Table 8). For example, the concrete grade was varied (10, 15, 20, etc.), while keeping everything else unchanged. Then the operation was repeated with the steel grade, returning the concrete to the starting conditions, and so on, until all variables were exhausted. After this first round of data collection, a similar procedure was followed, but changing two parameters at a time. Table 8 schematically illustrates some of the changes made.

4. Resolution of the problem through ANN

The structure of the ANN must be adapted to the specific problem, and it is therefore necessary to define the best setting to process the algorithm. Different tests were carried out with this aim, comparing each time the obtained results. In Fig. 8 it is shown the configuration that guaranteed the best accuracy, both for the know and predicted results. The ANN used for the study were developed using MATLAB's Deep Learning Tool Box plug-in Ref. [61].

The architecture of the network is based on the multilayer feed-forward type perceptron. Thus, it can approximate different types of functions, including integrable and continuous functions. As a setting for data processing, two hidden layers characterised by 10 neurons each and a sigmoid activation function (9) were chosen. The outputs, on the other hand, use a linear function (10).

$$f(x) = \frac{1}{1 + e^{-x}} \tag{9}$$

$$f(x) = x \tag{10}$$

To improve the network performance, Bayesian backpropagation regularisation was used as a training function. The algorithm reduces the combination of weights and errors (mean squared error) improving the ability to generalise the results at the end of the training. Moreover, it provides excellent results in the cases of quantitative studies, handling complex relationships, as illustrated by Kayri [62] who compared this procedure with the Levenberg-Marquardt algorithm.

The refinement of the ANN proceeded with the optimization of the exploited dataset. The wide range of values assumed by the parameters in absolute terms, with both high and low numbers (e.g., base shear expressed in kN and pseudo-acceleration in m/s^2) required an a priori normalization of the values. The traditional min-max algorithm was performed separately for each input and output value (11).

$$v' = \frac{v - min}{max - min} \tag{11}$$

where v' represent the normalised value, v the initial one and min and max are, respectively, the maximum and minimum values

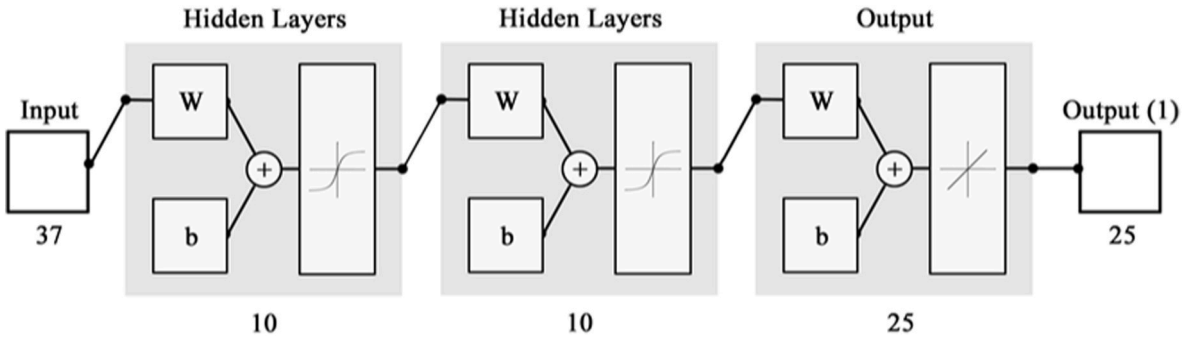

Fig. 8. Schematic representation of the system.

associated to the specific parameter.

Finally, in order to facilitate the convergence of the neural network and to vary the percentage of the dataset used in the ANN training test, the order of insertion of the rows of data was randomised, eliminating the possibility of incorrect associations of the prediction.

5. Results and discussion

The ANN validation was performed using k-fold cross-validation. This made it possible to optimise the database, exploiting all the data without losing important information during the analyses and systematically testing the results.

Furthermore, the collected data were analysed in a parallel study focused on the incidence of input parameters towards the seismic response of buildings. It was evaluated how some characteristics of the structure (concrete class, steel grade, etc.) can influence the seismic response of a generic RC building, confirming the results of previous studies (M. H [38]. The investigation lays the foundations for a future optimization of the research (e.g., by streamlining the procedure by excluding less relevant parameters) and aims at increasing the practitioner's awareness of the impact of certain variables on the global behaviour of a structure.

5.1. Assessment of the ANN through k-fold cross-validation

As mentioned above, in order to assess the predictive capabilities of the neural network used, it was decided to employ k-fold cross-validation. The method requires the dataset to be divided into k-subsets and was performed as listed below:

- training of the model considering k-1 folds (or partitions);
- validation of the results based on the left fold;
- repetition of the process until all subsets were used once as a sample for validation (k-times).

As shown in Table 9, the database was divided into 5 partitions (k = 5), each consisting of approximately 185 samples. In order to quantitatively compare the results predicted by the algorithm with the collected observation, a regression analysis was performed in which the Pearson coefficient (R) and the determination coefficient (R^2) were calculated for each partition. This evaluation was performed for the whole dataset (all), for the partition of samples never seen before by the ANN (test) and for the partitions used as training set (train).

$$R^2 = \left(\frac{\sum (x - m_x)(y - m_y)}{\sqrt{\sum (x - m_x)^2 \sum (y - m_y)^2}} \right)^2 \tag{12}$$

where x and y are two vectors of length n, and m_x and m_y are the mean values of x and y. Fig. 9 shows the distribution of results calculated with Matlab for iteration 1 in terms of Pearson's coefficient. As illustrated above, the box "train" refers to the training condition of the network (known values), the box "test" to the verification condition (unknown values), "all" considers all cases simultaneously.

Table 10 shows the determination coefficients (R^2) for the 17 outputs resulting from the five iterations. The separation between the three conditions: *train*, *test* and *all* was maintained.

The values obtained for the individual outputs in terms of R^2 denote in general very good network generalisation capabilities. Both the period of the structure and the base shear offer good results (0,88–0,98 for the tests and 0,95–0,98 for all the cases). On the other hand, the vulnerability index (I) is characterised by very low values denoting almost no correlation between observed and predicted values. This is probably caused by the nature of the parameter studied and by the variability of the input, characterised by a strong recurrence of the 0 value. The remaining parameters denote generalisation values of 0,72–0,98 with higher results for displacements in both x and y directions.

Table 11 shows the general Pearson's coefficient and the general coefficient of determination referred to each iteration in the three conditions *train*, *test,* and *all*.

In order to have a general measure of the network performance, the values shown in Table 12 were averaged using the Fisher transformation [63]. The following results were obtained from this operation.

It follows that the neural network manages to create a good correlation between the predicted and observed values when it comes to considering the totality of samples: the R value is equal to 0,971 and R^2 is 0,944, while, as expected, the value decreases for the previously unseen cases 0,938 (R) and 0,8814 (R^2).

Table 9
Schematic diagram of the k-fold cross-validation procedure.

Dataset – 928 Models					
Iteration 1	**Test**	Train	Train	Train	Train
Iteration 2	Train	**Test**	Train	Train	Train
Iteration 3	Train	Train	**Test**	Train	Train
Iteration 4	Train	Train	Train	**Test**	Train
Iteration 5	Train	Train	Train	Train	**Test**

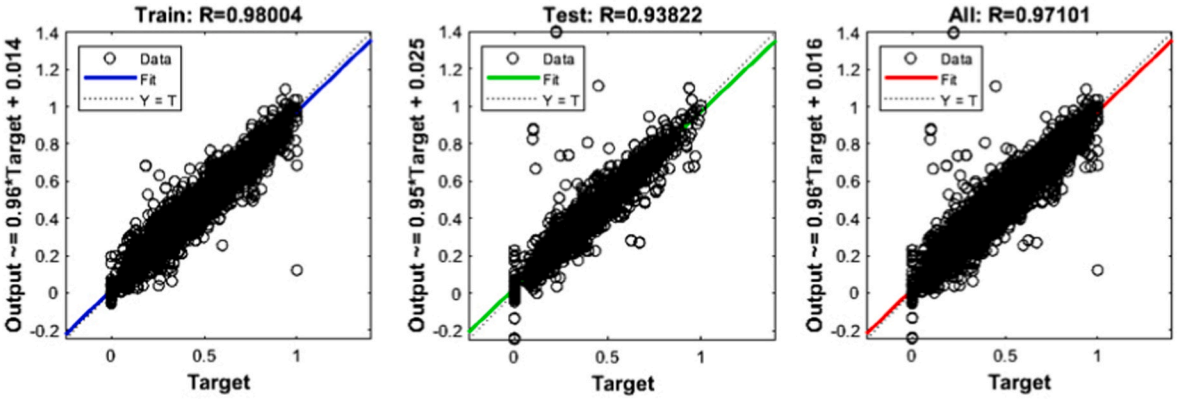

Fig. 9. Graphs referring to the Partition 1.

Table 10
Determination-coefficients for the 17 outputs in the five iterations.

	Iteration 1			Iteration 2			Iteration 3			Iteration 4			Iteration 5		
Outputs	Train	Test	All	Train	Test	All	Train	Test	All	Train	Test	All	Train	Test	All
$\mathbf{V_{LS\text{-}DL\text{-}x}}$	0,97	0,96	0,97	0,98	0,95	0,97	0,97	0,95	0,97	0,98	0,92	0,97	0,95	0,98	0,97
$\mathbf{V_{LS\text{-}SD\text{-}x}}$	0,98	0,96	0,97	0,98	0,95	0,97	0,98	0,93	0,97	0,98	0,94	0,97	0,93	0,98	0,97
$\mathbf{V_{LS\text{-}NC\text{-}x}}$	0,98	0,96	0,97	0,98	0,95	0,97	0,98	0,93	0,97	0,98	0,94	0,97	0,93	0,98	0,97
$\mathbf{m^*_x}$	0,70	0,75	0,71	0,69	0,66	0,68	0,71	0,61	0,69	0,67	0,66	0,67	0,50	0,63	0,60
$\mathbf{T_x}$	0,98	0,97	0,98	0,98	0,90	0,96	0,98	0,97	0,98	0,97	0,95	0,97	0,95	0,98	0,97
$\mathbf{d_{LS\text{-}DL\text{-}x}}$	0,86	0,76	0,84	0,85	0,78	0,84	0,86	0,78	0,84	0,87	0,83	0,86	0,78	0,87	0,85
$\mathbf{d_{LS\text{-}SD\text{-}x}}$	0,94	0,77	0,91	0,94	0,87	0,93	0,94	0,75	0,90	0,95	0,81	0,92	0,72	0,95	0,90
$\mathbf{d_{LS\text{-}NC\text{-}x}}$	0,94	0,76	0,91	0,94	0,87	0,93	0,94	0,75	0,90	0,95	0,81	0,92	0,73	0,95	0,90
$\mathbf{V_{LS\text{-}DL\text{-}y}}$	0,97	0,96	0,97	0,97	0,94	0,96	0,97	0,93	0,96	0,97	0,90	0,96	0,92	0,97	0,96
$\mathbf{V_{LS\text{-}SD\text{-}y}}$	0,98	0,97	0,98	0,98	0,95	0,97	0,98	0,94	0,97	0,98	0,92	0,97	0,92	0,98	0,96
$\mathbf{V_{LS\text{-}NC\text{-}y}}$	0,98	0,97	0,98	0,98	0,95	0,97	0,98	0,94	0,97	0,98	0,91	0,97	0,92	0,98	0,96
$\mathbf{m^*_y}$	0,72	0,83	0,74	0,72	0,66	0,71	0,73	0,74	0,73	0,72	0,69	0,71	0,48	0,71	0,63
$\mathbf{T_y}$	0,97	0,95	0,97	0,97	0,88	0,95	0,96	0,97	0,96	0,97	0,95	0,97	0,93	0,97	0,96
$\mathbf{d_{LS\text{-}DL\text{-}y}}$	0,88	0,73	0,85	0,88	0,69	0,83	0,86	0,74	0,84	0,90	0,73	0,85	0,64	0,90	0,83
$\mathbf{d_{LS\text{-}SD\text{-}y}}$	0,96	0,72	0,90	0,96	0,84	0,94	0,96	0,81	0,93	0,95	0,77	0,91	0,75	0,96	0,91
$\mathbf{d_{LS\text{-}NC\text{-}y}}$	0,96	0,72	0,90	0,96	0,84	0,94	0,96	0,81	0,93	0,95	0,76	0,91	0,75	0,97	0,91
I	0,13	0,08	0,12	0,14	0,06	0,13	0,17	0,10	0,16	0,10	0,42	0,18	0,02	0,12	0,10

Table 11
Correlation between predicted and observed outputs for each iteration.

	$\boldsymbol{R_{train}}$	$\boldsymbol{R_{test}}$	$\boldsymbol{R_{all}}$	$\boldsymbol{R^2_{train}}$	$\boldsymbol{R^2_{test}}$	$\boldsymbol{R^2_{all}}$
Iteration 1	0,980	0938	0,971	0,9604	0,8798	0,9428
Iteration 2	0,980	0952	0,974	0,9604	0,9063	0,9487
Iteration 3	0,980	0941	0,972	0,9604	0,8855	0,9448
Iteration 4	0,981	0935	0,972	0,9624	0,8742	0,9448
Iteration 5	0,981	0925	0,969	0,9624	0,8556	0,9390

5.2. Impact of parameters on vulnerability

The collection of data and their association with outputs allowed to conduct a parallel study on the impact of the inputs on the seismic response, evaluating the results obtained from the FEM modelling.

The investigation was carried out with reference to the acceleration to the limit state of significant damage in both directions for the Mechanical and Construction parameters, excluding the morphological ones, due to the high aleatory nature that characterises them. The acceleration at the limit state of significant damage is calculated as follows:

$$a_{LS} = \frac{V_{LS}}{g \cdot m^*} \tag{13}$$

where g is the acceleration of gravity and m^* is the activated mass.

An example is shown below, carried out on the concrete-class variations (Table 13). On IS 1–4, the percentages of variation of acceleration in the LS-SD were calculated for the different strength classes (10, 15, 20, etc.). Through a series of arithmetic averages

Table 12
Pearson coefficient (R) and determination coefficient (R^2) for the whole neural network.

	R_{train}	R_{test}	R_{all}	R^2_{train}	R^2_{test}	R^2_{all}
ANN	0,9804	0,9388	0,9716	0,9612	0,8814	0,9441

Table 13
Impact of parameters, concrete class.

	Rck	$a_{LS\text{-}SD\text{-}x}$	%	Δ	$a_{LS\text{-}SD\text{-}y}$	%	Δ
IS 1	30	0,08485	100%	0%	0,05882	100%	0%
	10	0,05941	70%	30%	0,04350	74%	26%
	15	0,06202	73%	27%	0,04168	71%	29%
	20	0,06676	79%	21%	0,04819	82%	18%
	25	0,07360	87%	13%	0,05301	90%	10%
	35	0,08867	105%	5%	0,06044	103%	3%
	60	0,10864	128%	28%	0,09507	162%	62%
	30	0,08485	100%	0%	0,05882	100%	0%
IS 2	30	0,11010	100%	0%	0,10020	100%	0%
	10	0	0%	100%	0	0%	100%
	15	0	0%	100%	0	0%	100%
	20	0,09899	90%	10%	0,10011	100%	0%
	25	0,09918	90%	10%	0,09798	98%	2%
	35	0,11555	105%	5%	0,10561	105%	5%
	50	0,12529	114%	14%	0,11318	113%	13%
	60	0,13131	119%	19%	0,12210	122%	22%
IS 3	30	0,11533	100%	0%	0,10571	100%	0%
	10	0,07439	65%	35%	0,07742	73%	27%
	15	0,06803	59%	41%	0,08848	84%	16%
	20	0,08539	74%	26%	0,09414	89%	11%
	25	0,10301	89%	11%	0,10014	95%	5%
	35	0,11889	103%	3%	0,10846	103%	3%
	50	0,13097	114%	14%	0,11660	110%	10%
IS 4	30	0,10729	100%	0%	0,11073	100%	0%
	10	0,07949	74%	26%	0,08232	74%	26%
	15	0,10659	99%	1%	0,10259	93%	7%
	20	0,10359	97%	3%	0,10697	97%	3%
	25	0,10270	96%	4%	0,10622	96%	4%
	35	0,10942	102%	2%	0,11245	102%	2%
	50	0,12246	114%	14%	0,12580	114%	14%
	60	0,12969	121%	21%	0,13266	120%	20%

aimed at normalising the results, an average percentage variation was obtained, which expresses the incidence of this input on the acceleration value.

The same assessment is made for all important input parameters (Fig. 10).

As expected, the investigation shows that the parameters most affected in the calculation of the seismic response are those related to the vertical resisting elements. In particular, the most significant parameter on the pseudo-acceleration value seems to be the size of the columns and their reinforcement percentage (C_x, C_y, $A_{s,c,trans}$ and $A_{s,c,long}$).

It can also be observed that the designated use and the degree of reinforcement of the beams (stirrups and longitudinal bars) although fundamental for the verification against vertical loads are less influent towards the horizontal actions.

It is also possible to observe a different impact of the parameters on the two directions considered: even if the relative ratios remain similar, there is a difference in absolute terms. For example, the size of the columns, which in both cases is the most important parameter, is more relevant in the y direction (48%) than in the x direction (38%). A similar behaviour is observed on the results obtained for the column reinforcement parameters. It is interesting to note that in the cases of less impactful parameters (beams and their reinforcement) the relative differences in the two directions are also minimal.

The only significant parameter on which the impact in the x-direction is greater than in the y-direction, although minimal, is the concrete strength.

6. Conclusions and further steps

The methodology illustrated in this article is based on interdisciplinary research work combining fields and results from structural engineering and statistics. This dualism of the process is what makes the difference from the classic methods (DPM, RVS, etc.) and where its real potential lies. After a collection of data, characterising the RC residential building stocks, focused on Bologna districts, but representative of the dominant building typology in most Italian and European city suburbs, a set of reference structures were determined. A database collecting the inputs and related outputs was then generated through FEM analyses performed on eight ISs.

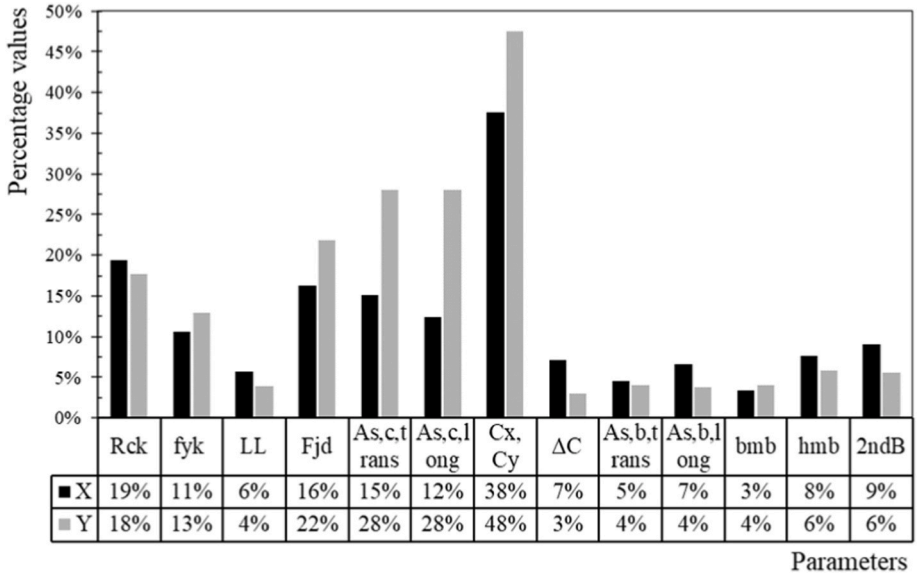

	Rck	fyk	LL	Fjd	As,c,trans	As,c,long	Cx, Cy	ΔC	As,b,trans	As,b,long	bmb	hmb	2ndB
X	19%	11%	6%	16%	15%	12%	38%	7%	5%	7%	3%	8%	9%
Y	18%	13%	4%	22%	28%	28%	48%	3%	4%	4%	4%	6%	6%

Fig. 10. Impact of parameters, direction x (above) and direction y (below).

Based on this database, the neural network was first created and then optimised using the most suitable settings to solve the problem. Through k-fold cross-validation procedure, the ANN training was finally improved and simultaneously verified, showing a relevant predictive capacity. Considering the totality of the samples (*all*), the coefficient of determination stood at a value of 0,94, with a Pearson coefficient of 0,97. With reference to previously unseen cases (*test*) the correlation between predicted and observed values indicated an R^2 of 0,88 and an R of 0,93.

Although the study reported here testifies to the effectiveness of the method, it also confirms also that the accuracy of the ANN is highly dependent on the number and variety of models included in the dataset and that the variations included in the training are still not sufficient to cover all existing building types in RC. The results illustrated for the single outputs also show an uneven predictive capacity of the network: while most of the parameters have high correlation values (especially the period of the structure and the base shear), the vulnerability index (I) seems unsuitable for the type of approach adopted and will have to be redesigned in future updates of the work.

The authors' intention was to validate the procedure as a method to create a prioritising tool capable of identifying, on a large scale, the most vulnerable buildings among some recurrent typologies. Furthermore, the parameters determining the ISs were chosen in such a way as to allow the database to be expanded in subsequent phases. This possibility would allow an increase in the accuracy of the ANN as well as a greater coverage of the building typologies also with reference to different territorial areas. The study carried out suggests that in the future it will be possible to create a method, based on this preliminary system, capable of covering the majority of RC structures whose vulnerability can be determined in a few steps.

Finally, a parallel study on the impact of specific construction parameters on the performance of RC moment-resisting frames against horizontal loads is also reported as a further contribute to the framework concerning vulnerability assessment of RC buildings.

With the aim of prioritising the buildings at higher seismic risk, assisting decision makers in the implementation of seismic risk reduction strategies, and the undeniable advantage of reducing the time and cost of structural analysis, the large-scale application of rapid seismic vulnerability assessment methods will play a key role in the years to come.

Declaration of competing interest

The authors declare that they have no known competing financial interests or personal relationships that could have appeared to influence the work reported in this paper.

Acknowledgements

This article is part of the Pro-GET-onE project which has received funding from the European Union's Horizon 2020 Innovation action under grant agreement No 723747.

Appendix A

The complete list of parameters used as inputs in the creation of the database is given below in Table 14. The designation of the values is given in Section 2.2.

Table 14
List of parameters used as inputs in the database.

	Designation	Provided variables	U.M.
Mechanical Parameters			
1	$\mathbf{R_{ck}}$	10; 15; 20; 25; 30; 35; 50; 60	N/mm^2
2	$\mathbf{f_{yk}}$	220; 320; 380; 440; 450	N/mm^2
Construction Parameters			
3	$\mathbf{C_x}$	0,25; 0,30; 0,35; 0,40; 0,45; 0,50; 0,55; 0,60; 0,65	m
4	$\mathbf{C_y}$	0,25; 0,30; 0,35; 0,40; 0,45; 0,50; 0,55; 0,60; 0,65	m
5	$\mathbf{A_{s,c,long}}$	452; 616; 804; 923; 1.018; 1.206; 1.256; 1.526; 1.884; 2.280; 3.770; 4.562	mm^2
6	$\mathbf{A_{s,c,trans}}$	226; 283; 396; 402; 503; 565; 670; 704; 1.005; 1.169; 1.371; 1.571; 2.827; 3.789; 5.655	mm^2/ m
7	**ΔC**	0; 1	–
8	$\mathbf{h_{mb}}$	0,35; 0,40; 0,45; 0,50; 0,55; 0,60; 0,65; 0,70	m
9	$\mathbf{b_{mb}}$	0,20; 0,25; 0,30; 0,35; 0,40; 0,45; 0,50	m
10	$\mathbf{A_{s,b,long}}$	282; 424; 528; 565; 646; 678; 740; 762; 807; 833; 847; 925; 932; 968; 983; 1.018; 1.055; 1.070; 1.110; 1.130; 1.203; 1.475; 1.582	mm^2
11	$\mathbf{A_{s,b,trans}}$	703; 785; 1.047; 1.090; 1.100; 1.280; 1.340; 1.583; 1.649; 1.727	mm^2/ m
12	**w**	0; 1	–
13	**LL**	2; 3; 4	kN/m^2
14	$\mathbf{F_{jd}}$	0; 1	–
15	$\mathbf{2^{nd}B}$	0; 1	–
16	**DC**	0; 1	–
Morphological parameters			
17	**BA**	120; 123,5; 130; 135; 136,5; 140; 143; 150; 156; 162,5; 169; 175,5; 182; 195; 230; 300	m^2
18	**BP**	44; 45; 46; 47; 48; 50; 51; 52; 53; 54; 56; 66; 72	m
19	$\boldsymbol{J_{min}}$	1.440; 1.628; 1.739; 1.831; 1.922; 2.014; 2.050; 2.197; 2.287; 2.289; 2.380; 2.665; 2.813; 2.973; 3.656; 10.139; 13.181	m^4
20	$\boldsymbol{J_{max}}$	928; 1.000; 1.042; 1.083; 1.125; 1.167; 1.250; 1.442; 1.872; 1.917; 2.116; 2.380; 2.472; 2.563; 2.746; 4.210	m^4
21	**N°C**	12; 15; 16; 24	–
22	$\mathbf{l_{x,min}}$	3,0	m
23	$\mathbf{l_{x,max}}$	4,5; 5,0; 5,5; 6,0; 6,5	m
24	$\mathbf{l_{y,max}}$	3,0; 4,0	m
25	$\mathbf{l_{y,min}}$	5,0; 5,5; 6,0; 6,5; 7,0	m
26	$\mathbf{M_{l,x}}$	4,0; 4,2; 4,3; 4,5; 4,6; 4,7; 4,9	m
27	$\mathbf{M_{l,y}}$	4,1; 4,2; 4,3; 4,4; 4,5; 4,6; 4,8; 5,0; 5,3	m
28	$\boldsymbol{\sigma_{l,x}}$	0,71; 0,77; 0,80; 0,82; 0,85; 0,94; 1,08; 1,18; 1,23; 1,25; 1,41	–
29	$\boldsymbol{\sigma_{l,y}}$	0,75; 0,85; 0,94; 1,00; 1,08; 1,25; 1,25; 1,33; 1,50; 2,09	–
30	$\mathbf{IR_x}$	0,66; 0,85; 0,96; 1	–
31	$\mathbf{IR_y}$	0,71; 0,75; 0,81; 0,93; 0,95; 1	–
32	**N°St**	2; 3; 4; 5; 6; 8	–
33	$\mathbf{h_{is,min}}$	3; 3,5	m
34	$\mathbf{h_{is,max}}$	3,5	m
35	$\mathbf{M_{h,is}}$	3; 3,05; 3,08; 3,12; 3,16; 3,25; 3,5	m
36	$\boldsymbol{\sigma_{h,is}}$	0; 0,16; 0,17; 0,18; 0,19; 0,20; 0,21; 0,23; 0,25	–
37	$\mathbf{H_{tot}}$	6,5; 9,5; 12,5; 15,0; 15,5; 17,5; 18,5; 24,5	m

Appendix B

Some tests carried out with more traditional prediction methods, which generally allow for greater interpretability of the results provided, have shown low predictive capabilities even in relation to known cases. Specifically, the tests were carried out on three simple linear regression models with logarithmic transformation of the values. The transformations concerned in one case the domain values, in another the codominant values and finally both (domain and codominant). A summary table comparing the 3 linear regression models is given in terms of the coefficient of determination (Table 15).

Table 15
Coefficient of determination for linear regressions

Target output	$\boldsymbol{R^2_{dom}}$	$\boldsymbol{R^2_{cod}}$	$\boldsymbol{R^2_{dom-cod}}$
$\mathbf{V_{LS\text{-}DL\text{-}x}}$	0,806	0560	0,559
$\mathbf{V_{LS\text{-}SD\text{-}x}}$	0,800	0561	0,568
$\mathbf{V_{LS\text{-}NC\text{-}x}}$	0,799	0561	0,567
$\mathbf{m^*_x}$	0,729	0759	0,681
$\mathbf{T_x}$	0,875	0953	0,955
$\mathbf{d_{LS\text{-}DL\text{-}x}}$	0,743	0449	0,454

(*continued on next page*)

Table 15 (*continued*)

Target output	R^2_{dom}	R^2_{cod}	$R^2_{dom-cod}$
$\mathbf{d_{LS\text{-}SD\text{-}x}}$	0,630	0519	0,541
$\mathbf{d_{LS\text{-}NC\text{-}x}}$	0,626	0518	0,539
$\mathbf{V_{LS\text{-}DL\text{-}y}}$	0,755	0568	0,532
$\mathbf{V_{LS\text{-}SD\text{-}y}}$	0,781	0582	0,561
$\mathbf{V_{LS\text{-}NC\text{-}y}}$	0,780	0581	0,559
$\mathbf{m^*_y}$	0,934	0968	0,941
$\mathbf{T_y}$	0,832	0909	0,903
$\mathbf{d_{LS\text{-}DL\text{-}y}}$	0,511	0306	0,296
$\mathbf{d_{LS\text{-}SD\text{-}y}}$	0,482	0475	0,419
$\mathbf{d_{LS\text{-}NC\text{-}y}}$	0,480	0474	0,417
I	0,099	0079	0,060

The mean values of all three models are well below 1, showing a poor generalisation capacity.

References

[1] Domenico Giardini, Jochen Woessner, Laurentiu Danciu, Mapping Europe's seismic hazard, Eos Trans. Am. Geophys. Union 95 (2014), https://doi.org/10.1002/2014EO290001.

[2] University of Bologna, ABT Consulting Engineering, Technical University of Munich, and National and Kapodistrian University of Athens, 2017. D2.2: Report on Structural and Seismic Retrofit Techniques and Projects. Pro-GET-onE.

[3] Seong-Hoon Jeong, Amr Elnashai, Probabilistic fragility analysis parameterized by fundamental response quantities, Eng. Struct. 29 (2007) 1238–1251, https://doi.org/10.1016/j.engstruct.2006.06.026.

[4] Oh-Sung Kwon, Amr Elnashai, The effect of material and ground motion uncertainty on the seismic vulnerability curves of RC structure, Eng. Struct. 28 (2006) 289–303, https://doi.org/10.1016/j.engstruct.2005.07.010.

[5] Vitor Silva, Sinan Akkar, Jack Baker, Paolo Bazzurro, José Miguel Castro, Helen Crowley, Matjaz Dolsek, Carmine Galasso, Sergio Lagomarsino, Ricardo Monteiro, Daniele Perrone, Kyriazis Pitilakis, Dimitrios Vamvatsikos, Current challenges and future trends in analytical fragility and vulnerability modeling, Earthq. Spectra 35 (4) (2019) 1927–1952, https://doi.org/10.1193/042418eqs101o.

[6] D. Benedetti, V. Petrini, Sulla vulnerabilità sismica di edifici in muratura: un metodo di valutazione, L'industria delle costruzioni 149 (1984) 66–74.

[7] P. Angeletti, A. Bellina, E. Guagenti, A. Moretti, V. Petrini, Comparison between vulnerability assessment and damage index, some results, in: 9th World Conference on Earthquake Engineering, Tokyo-Kyoto, Japan, 1988.

[8] V. Petrini, E. Guagenti, Il caso delle vecchie costruzioni: verso una nuova legge danni-intensità, in: 4th Italian National Conference on Earthquake Engineering, Milan, Italy, 1989.

[9] A. Corsanego, V. Petrini, Seismic vulnerability of buildings - work in progres, in: 2nd Workshop on Seismic Risk Vulnerability and Risk Assessment, Trieste, Italy, 1990.

[10] Gruppo Nazionale per la Difesa dai Terremoti, GNDT-SSN, Scheda di esposizione e vulnerabilità e di rilevamento danni di primo e secondo livello (muratura o c. a.), Gruppo Nazionale per la Difesa dai Terremoti, Rome, Italy, 1994.

[11] A. Bernardini, Qualitative and Quantitative Measures in Seismic Damage Assessment and Forecasting of Masonry Buildings, 1998 (International Workshop on Measures of Seismic Damage to Masonry Buildings, Monselice, Italy).

[12] F. Braga, M. Dolce, D. Liberatore, A statistical study on damaged buildings and an ensuing review of the MSK/76 scale, in: 7th European Conference on Earthquake Engineering, Athens, 1982.

[13] F D Liberatore Braga, M. Dolce, Fast and reliable damage estimations for optimal relief operations, in: Int. Symp. On Earthquake Relief in Less Industrialized Areas, Zurich, 1984.

[14] Sergio Ruggieri, Chiara Tosto, Giulia Rosati, Giuseppina Uva, Giuseppe Andrea Ferro, Seismic vulnerability analysis of masonry churches in piemonte after 2003 Valle Scrivia earthquake: post-event screening and situation 17 Years later, Int. J. Architect. Herit. 51 (2020) 1–29, https://doi.org/10.1080/15583058.2020.1841366, 0.

[15] Ciriaco Chinni, Claudio Mazzotti, Marco Savoia, Gianluca Perri, RE.SIS.TO: una metodologia speditiva per la valutazione di vulnerabilità sismica di edifici in muratura e calcestruzzo armato, in: XV Convegno ANIDIS - L'Ingegneria Sismica in Italia, Padua, Italy, 2013.

[16] Sergio Ruggieri, Daniele Perrone, Marianovella Leone, Giuseppina Uva, Maria Antonietta Aiello, A prioritization RVS methodology for the seismic risk assessment of RC school buildings, Int. J. Disaster Risk Reduct. 51 (2020), 101807, https://doi.org/10.1016/j.ijdrr.2020.101807.

[17] B. Lizundia, S. Durphy, M. Griffin, W. Holmes, A. Hortacsu, B. Kehoe, K. Porter, B. Welliver, Third Edition update of FEMA P-154: rapid visual screening for potential seismic hazards, in: Improving the Seismic Performance of Existing Buildings and Other Structures 2015, 2015, pp. 775–786.

[18] World Health Organization (WHO), and Organization Pan American Health, Hospital Safety Index: Guide for Evaluators, second ed., World Health Organization, Geneva, 2015.

[19] Giacomo Di Pasquale, Giampiero Orsini, Roberto W. Romeo, New developments in seismic risk assessment in Italy, Bull. Earthq. Eng. 3 (1) (2005) 101–128, https://doi.org/10.1007/s10518-005-0202-1.

[20] M.H. Arslan, M. Ccylan, T. Koyuncu, An ann approaches on estimating earthquake performances of existing RC buildings, Neural Netw. World 22 (5) (2012) 443–458, https://doi.org/10.14311/NNW.2012.22.027.

[21] Ahmet Yakut, Guney Ozcebe, M. Yucemen, A Statistical Procedure for the Assessment of Seismic Performance of Existing Reinforced Concrete Buildings in Turkey, 2020.

[22] P. Gülkan, M.A. Sozen, Procedure for determining seismic vulnerability of building structures, ACI Struct. J. 96 (3) (1999) 336–342.

[23] Hasan Boduroglu, Pinar Ozdemir, Alper Ilki, Semra Sirin, Cem Demir, Fatma Baysan, Towards a modified rapid screening method for existing medium rise RC buildings in Turkey, in: 13th World Conference on Earthquake Engineering, 2004, pp. 1–6.

[24] Sevcan Tezcan, İhsan Bal, Fatma Gulay, P25-Scoring method for the collapse vulnerability assessment of R/C buildings, J. Chin. Inst. Eng. 34 (2011) 769–781, https://doi.org/10.1080/02533839.2011.591548.

[25] Colin Camerer, Eric Johnson, The Process-Performance Paradox in Expert Judgment - How Can Experts Know So Much and Predict So Badly?, 1991.

[26] Gary Klein, Conditions for intuitive expertise A failure to disagree, Am. Psychol. 64 (2009) 515–526, https://doi.org/10.1037/a0016755.

[27] Y.L. Mo, H.Y. Hung, J. Zhong, Investigation of stress-strain relationship of confined concrete in hollow bridge columns using neural networks, J. Test. Eval. 30 (4) (2002) 330–339.

[28] C.H. Jeng, Y.L. Mo, Quick seismic response estimation of prestressed concrete bridges using artificial neural networks, J. Comput. Civ. Eng. 18 (4) (2004) 360–372, https://doi.org/10.1061/(ASCE)0887-3801(2004)18:4(360).

[29] V. Giri, A. Upadhyay, ANN based prediction of moment coefficients in slabs subjected to patch load, Struct. Eng. Mech. 24 (4) (2006) 509–514, https://doi.org/10.12989/sem.2006.24.4.509.

[30] M. Hakan Arslan, Predicting of torsional strength of RC beams by using different artificial neural network algorithms and building codes, Adv. Eng. Software 41 (7) (2010) 946–955, https://doi.org/10.1016/j.advengsoft.2010.05.009.

[31] M.H. Arslan, M. Ceylan, M.Y. Kaltakci, Y. Ozbay, F.G. Gulay, Prediction of force reduction factor (R) of prefabricated industrial buildings using neural networks, Struct. Eng. Mech. 27 (2) (2007) 117–134, https://doi.org/10.12989/sem.2007.27.2.117.

[32] H.N. Cho, Y.M. Choi, S.C. Lee, C.K. Hur, Damage assessment of cable stayed bridge using probabilistic neural network, Struct. Eng. Mech. 17 (3–4) (2004) 483–492.

[33] Jong Jae Lee, Jong Won Lee, Jin Hak Yi, Chung Bang Yun, Hie Young Jung, Neural networks-based damage detection for bridges considering errors in baseline finite element models, J. Sound Vib. 280 (3) (2005) 555–578, https://doi.org/10.1016/j.jsv.2004.01.003.

[34] D. Sabia, A. De Stefano, L. Sabia, Probabilistic neural networks for seismic damage mechanisms prediction, Earthq. Eng. Struct. Dynam. 28 (7–8) (1999) 807–821.

[35] S. Chang, D. Kim, C. Chang, S.G. Cho, Active response control of an offshore structure under wave loads using a modified probabilistic neural network, J. Mar. Sci. Technol. 14 (2) (2009) 240–247, https://doi.org/10.1007/s00773-008-0040-3.

[36] D.H. Kim, D. Kim, S. Chang, Application of lattice probabilistic neural network for active response control of offshore structures, Struct. Eng. Mech. 31 (2) (2009) 153–162, https://doi.org/10.12989/sem.2009.31.2.153.

[37] Dookie Kim, Kim Dong, Jintao Cui, Hyeong Seo, Young Lee, Iterative neural network strategy for static model identification of an FRP deck, Steel Compos. Struct. 9 (2009), https://doi.org/10.12989/scs.2009.9.5.445.

[38] M.H. Arslan, An evaluation of effective design parameters on earthquake performance of RC buildings using neural networks, Eng. Struct. 32 (7) (2010) 1888–1898, https://doi.org/10.1016/j.engstruct.2010.03.010.

[39] M.H. Arslan, Application of ANN to evaluate effective parameters affecting failure load and displacement of RC buildings, Nat. Hazards Earth Syst. Sci. 9 (3) (2009) 967–977.

[40] O.R. De Lautour, P. Omenzetter, Prediction of seismic-induced structural damage using artificial neural networks, Eng. Struct. 31 (2) (2009) 600–606, https://doi.org/10.1016/j.engstruct.2008.11.010.

[41] Vazirizade, Sayyed Mohsen, Saeed Nozhati, Mostafa Allamehzadeh, Seismic reliability assessment of structures using artificial neural network, J. Build Eng. 11 (2017), https://doi.org/10.1016/j.jobe.2017.04.001.

[42] Stefano Bonini, Giuliana Caivano, Probability of Default Modeling: A Machine Learning Approach, 2018.

[43] Konstantinos Morfidis, Konstantinos Kostinakis, Approaches to the rapid seismic damage prediction of r/c buildings using artificial neural networks, Eng. Struct. 165 (2018), https://doi.org/10.1016/j.engstruct.2018.03.028.

[44] Tiago Ferreira, João Estêvão, Rui Maio, Romeu Vicente, The use of Artificial Neural Networks to estimate seismic damage and derive vulnerability functions for traditional masonry, Front. Struct. Civ. Eng. (2020), https://doi.org/10.1007/s11709-020-0623-6.

[45] João Estêvão, Feasibility of using neural networks to obtain simplified capacity curves for seismic assessment, Buildings 8 (2018) 151, https://doi.org/10.3390/buildings8110151.

[46] Dr Abbes Berrais, Artificial neural networks in structural engineering: concept and applications : تطبيقات الشبكات العصبية الاصطناعية في العندسة الانشائية المفهوم والحالة الراهنة, J. King Abdulaziz Univ. Eng. Sci. 12 (1999) https://doi.org/10.4197/Eng.12-1.4.

[47] Giulio Russo, Metodi speditivi per la valutazione del comportamento strutturale di edifici intelaiati in c.a. mediante l'applicazione di reti neurali. Studio dell'influenza delle caratteristiche meccaniche e geometriche: analisi e valutazione dei risultati, Single Cycle Degree/Combined Bachelor and Master in Architecture and Building Engineering Master Thesis, Department of Architecture, Alma Mater Studiorum, University of Bologna, 2019, https://amslaurea.unibo.it/id/eprint/17901.

[48] Valentina Gnucci, Metodi speditivi per la valutazione del comportamento strutturale di edifici intelaiati in c.a. mediante l'applicazione di reti neurali. Studio dell'influenza delle caratteristiche meccaniche e geometriche: scelta dei parametri di analisi, Single Cycle Degree/Combined Bachelor and Master in Architecture and Building Engineering Master Thesis, Department of Architecture, Alma Mater Studiorum, University of Bologna, 2019, https://amslaurea.unibo.it/id/eprint/17902.

[49] Lorenzo Stefanini, Metodi speditivi per la valutazione del comportamento strutturale degli edifici intelaiati in calcestruzzo armato: studio dell'influenza delle caratteristiche costruttive mediante applicazione di reti neurali, Single Cycle Degree/Combined Bachelor and Master in Architecture and Building Engineering Master Thesis, Department of Architecture, Alma Mater Studiorum, 2016, https://amslaurea.unibo.it/id/eprint/12504.

[50] European Commitee for Standardization (CEN), EN 1998-3: Eurocode 8: Design of Structures for Earthquake Resistance - Part 3: Assessment and Retrofitting of Buildings, 2005 (Brussels, Belgium).

[51] Ministero dei Lavori Pubblici, Norme per l'accettazione dei leganti idraulici, Gazzetta Ufficiale, Rome, Italy, 1939.

[52] Ministero dei Lavori Pubblici, Norme tecniche alle quali devono uniformarsi le costruzioni in conglomerato cementizio, normale e precompresso ed a struttura metallica, Gazzetta Ufficiale n, Roma, Italy, 1972, p. 190.

[53] Ministero dei Lavori Pubblici, Norme tecniche per il calcolo, l'esecuzione ed il collaudo delle strutture in cemento armato, normale e precompresso e per le strutture metalliche, 1996. Rome, Italy: Suppl. Ord. alla Gazzetta Ufficiale n.29 del 5 febbraio 1996.

[54] Ministero delle Infrastrutture e dei Trasporti, Norme tecniche per le costruzioni, Gazzetta Ufficiale della Repubblica Italiana, 2008.

[55] European Commitee for Standardization (CEN), EN 1991-1-1: Eurocode 1: Actions on Structures - Part 1-1: General Actions - Densities, Self-Weight, Imposed Loads for Buildings, 2002 (Brussels, Belgium).

[56] CSI, SAP2000 Ultimate v21.2.0. Structural Analysis Program, Computer & Structures Inc, Berkeley (CA, USA), 2019.

[57] European Commitee for Standardization (CEN), EN 1992-1-1: Eurocode 2: Design of Concrete Structures - Part 1-1: General Rules and Rules for Buildings, 2004 (Brussels, Belgium).

[58] European Commitee for Standardization (CEN), EN 1998-1: Eurocode 8: Design of Structures for Earthquake Resistance - Part 1: General Rules, Seismic Actions and Rules for Buildings, 2004 (Brussels).

[59] Ministero delle Infrastrutture e dei Trasporti, Istruzioni per l'applicazione dell'«Aggiornamento delle "Norme tecniche per le costruzioni"» di cui al decreto ministeriale 17 gennaio 2018, Gazzetta Ufficiale della Repubblica Italiana, Rome, Italy, 2019.

[60] Ministero delle Infrastrutture e dei Trasporti, Norme tecniche per le costruzioni, Gazzetta Ufficiale della Repubblica Italiana, Rome, Italy, 2018.

[61] Matlab, Natick, The MathWorks Inc, Massachussetts, 2018.

[62] Murat Kayri, Predictive abilities of Bayesian regularization and Levenberg–Marquardt algorithms in artificial neural networks: a comparative empirical study on social data, Math. Comput. Appl. 21 (2016) 1–11, https://doi.org/10.3390/mca21020020.

[63] R.A. Fisher, Frequency distribution of the values of the correlation coefficients in samples from an indefinitely large population, Biometrika 10 (4) (1915) 507–521, https://doi.org/10.1093/biomet/10.4.507.